Supplementary Material

Discrimination of Euro 5 gasoline vs. Diesel light-duty engine primary and secondary particle emissions using multivariate statistical analysis of high-resolution mass spectrometry (HRMS) fingerprint

Camille Noblet[1,2], Francois Lestremau[1,3], Adrien Dermigny[1], Nicolas Karoski[1], Claudine Chatellier[1], Jérôme Beaumont[1], Yao Liu[4], Boris Vansevenant[4], Jean-Luc Besombes[2], and Alexandre Albinet[1]

[1]Institut National de l'Environnement industriel et des RISques (Ineris), 60550 Verneuil en Halatte, France
[2]Université Savoie Mont-Blanc, EDYTEM, 73000 Chambéry, France
[3]HSM, Univ Montpellier, IMT Mines Ales, CNRS, IRD, Ales, France[4]Université Gustave Eiffel, Univ Lyon, AME-EASE, F-69675 Lyon, France

Correspondence to: Alexandre Albinet (alexandre.albinet@ineris.fr) and Francois Lestremau (francois.lestremau@mines-ales.fr)

17   **1 Vehicle tested, driving cycles and fuels**

18   **Table S1. Characteristics of the two tested vehicles.**

Vehicle	N°1	N°2
Type	1.4 TSI, 16V DSG7, ID	1.6 HDI[c]
Fuel	Gasoline	Diesel
Standard	Euro 5	Euro 5
Empty weight (kg)	1285	1080
Mileage (km)	92550	105823
Gearbox (number of gears)	Sequential (7)	Manual (5)
Post treatment system	TWC[a]	DOC + Additive DPF[b]
In-service date	10/21/2009	10/30/2013

19   [a]TWC: Three-way catalysis

20   [b]DOC + Additive DPF: Diesel Oxidation Catalyst + Additive Diesel Particulate Filter

21   [c]HDI: High pressure direct injection

23   **Table S2. Main characteristics of the fuel used for the tested vehicles.**

	Diesel B7	Gasoline SP95-E10
Color	yellow	
Density at 15 °C (kg m^{-3})	833.4	739.4
Sulphur content (mg kg^{-1})	9.7	8.7
Water content (mg kg^{-1})	100	
Total contamination (mg kg^{-1})	< 12	
Total aromatic hydrocarbons (% m)	27.8	
Polycyclic aromatic hydrocarbons (% m)	4.7	
Lead content (mg L^{-1})	---	< 2.5
Manganese content (mg L^{-1})	---	< 5.0
Benzene content (% m)	---	0.61
Ethanol content (% vol)	---	7.3
ETBE content (% vol)	---	5.74
Total oxygenated compounds (% vol)	---	13.29
Oxygen content (% m)	---	3.7
Aromatic content (% vol)	---	22.2
Olefin content (% vol)	---	15.3
Saturated content (% vol)	---	49.3

26   **2 Sampling setup**

27   **Table S3. Overview of all instruments used to measure the gas- and particulate-phase pollutants for the experiments.**

Measured parameters	Phase	Sampling location	Instrument	Note
O_2	Gas	Emission and after dilution	Multigas analyzer PG250 (Horiba) Range: 0–25% in volume	Online
CO	Gas	Emission and after dilution	Multigas analyzer PG250 (Horiba) Range: 0–1000 ppm	Online
NO/NO_x	Gas	Emission	Multigas analyzer PG250 (Horiba) Range: 0–100 ppm	Online
		After dilution	Model 42i ($NO-NO_2-NO_x$) Analyzer (Thermo) Range: 0–100 ppm	
CO_2	Gas	Emission	VA 3000 (Horiba) Range: 0–10000 ppm	Online
		After dilution	VA 3000 (Horiba) Range: 0–5000 ppm	
SO_2	Gas	After dilution	AF 21 M Environnement S.A. Range: 0–0.05 ppm	Online
O_3	Gas	After dilution	Model 202, 2B Technologies Range: 0–250 ppm	Online
Particle number	Particle	After dilution	CPC Grimm Serie 5.400 Range: 5-1000 nm CPC TSI 3775 Range: 4–1000 nm	Online
Non-refractory PM chemical composition	Particle	After dilution	Time of Flight-Aerosol Chemical Speciation Monitor (ToF-ACSM) Aerodyne Research Range: 40–1000 nm	Online

3 Non-target screening analyses

Table S4. List of solvents and chemicals used (suppliers and purity).

Compound	Supplier	Purity (%)
Extraction and injection internal standards		
Beflubutamid-d$_7$	HPC Standards	99.8
Metsulfuron-d$_3$	HPC Standards	99.6
Succinic acid-d$_4$	CDN Isotopes	99.0
Nonanedioic acid-d$_{14}$	CDN Isotopes	99.0
^{13}C-Sulfamethazine	Sigma Aldrich	99.9
Simazine-d$_{10}$	Dr Ehrenstorfer	98.1
Diuron-d$_6$	Dr Ehrenstorfer	99.6
^{13}C-Diclofenac	Dr Ehrenstorfer	97.7
9,10-Anthraquinone-d$_8$	CDN Isotopes	99.0
1-Nitronaphthalene-d$_7$	CDN Isotopes	98.3
Benzo[g,h,i]perylene-d$_{12}$	CDN Isotopes	99.4
Pentadecane-d$_{32}$	Sigma Aldrich	98.0
Pentacosane-d$_{52}$	CDN Isotopes	98.6
Naphthalène-d$_8$	Supelco	99.9
2,2',5,5'-tetrachlorobiphenyl ^{13}C$_{12}$ (PCB52*)	Wellington	98.0
Perylene-d$_{12}$	Cambridge Isotope Laboratories	99.0
Solvents		
Acetonitrile	Honeywell, Merck	99.9
Methanol	Honeywell, Merck	99.9
Acetic acid	Fischer Chemical	LC/MS Grade
Ammonium acetate	Fischer Chemical	LC/MS Grade
Water	Millipore	Milli-Q (18 MΩ)

Table S5. Internal standard solutions with concentrations of compounds (µg mL^{-1}), mass, and retention time.

Internal standard	Concentration (µg mL^{-1})	Ionisation mode	Molecular mass (Da)	Retention time (RT, min)
LC				
Beflubutamid-d$_7$	0.5	+/−	362.1635	16.74
Metsulfuron-d$_3$	0.5	+/−	384.0931	10.66
Succinic acid-d$_4$	5	−	122.0517	0.94
Nonanedioic acid-d$_{14}$	5	−	202.1927	10.41
^{13}C-Sulfamethazine	5	+	293.2900	7.24
GC				
9,10-Anthraquinone-d$_8$	1		216.1026	20.60
1-Nitronaphthalene-d$_7$	1		180.0916	16.60
Benzo[g,h,i]perylene-d$_{12}$	1		288.1692	30.56
Pentadecane-d$_{32}$	0.05		244.4513	14.99
Pentacosane-d$_{52}$	1		404.7333	24.81
Naphthalene-d$_8$	0.1		136.1128	11.04
2,2',5,5'-tetrachlorobiphenyl ^{13}C$_{12}$ (PCB52*)	0.05		301.9626	20.29
Perylene-d$_{12}$	1		264.1692	28.18

38   **Table S6. Injection internal standard solutions with molecular mass and retention time.**

Internal standard	Ionisation mode	Molecular mass (Da)	Retention time (RT, min)
LC			
Simazine-d_{10}	+	211.1409	11.95
Diuron-d_6	+/−	238.0547	13.69
^{13}C-Diclofenac	+/−	301.0368	15.61
GC			
9-Fluorenone-d_9		212.1410	18.16
Phenanthrene d_{10}		188.1410	18.5

39

40   **Table S7. Chromatographic elution gradient for LC-HRMS.**

Time (min)	Mobile phase A (%)	Mobile phase B (%)
0	98	2
2	98	2
9	60	40
20	2	98
25	2	98

41

42   **Table S8. QToF parameters for both ionization modes used.**

		ESI (+)	ESI (−)
Source parameters	Sheath gas temperature (°C)	300	300
	Sheath gas flow (L/min)	13	13
	Nebulization pressure (psig)	30	30
	Capillary tension (V)	3500	3500
	Auxiliary gas temperature (°C)	200	200
	Auxiliary gas flow (L/min)	15	15
Acquisition parameters	Mass range (m/z)	70–3200	70–3200
	Calibration references	121.0508; 922.0098	112.9855; 1033.9881
	Scan number (spectra/min)	4	4
	IFunnel (V)	Funnel Exit DC: 50 Funnel RF HP: 200 Funnel RF LP: 100	Funnel Exit DC: 50 Funnel RF HP: 200 Funnel RF LP: 100

43
44
45
46
47
48
49
50
51
52
53

54 **Table S9. GC-QToF operating conditions.**

Parameters		EI	NICI
GC	Injection type	Pulsed splitless	
	Injection pulse pressure (psi)	50	
	Injection temperature (°C)	300	
	Carrier gas flow rate (He, mL min^{-1})	1.2	
	Transfer line temperature (°C)	280	
	Quench gas flow rate (He, mL min^{-1})	4	
	Gas collision flow rate (N$_2$, mL min^{-1})	1	
Oven programming	Initial temperature (°C); hold time (min)	40; 1.8	
	Temperature rate (°C min^{-1})	10	
	Final temperature (min); hold time (min)	325; 10	
	Total (min)	40.3	
QToF	Ionisation energy (eV)	70	70
	Source temperature (°C)	280	185
	Solvent delay (min)	6.5	-
	Reactant gas	-	CH$_4$ (99.999%)
	Mass range (m/z)	20–600	-

55

56 **4 Quality assurance and controls**

57

58
59
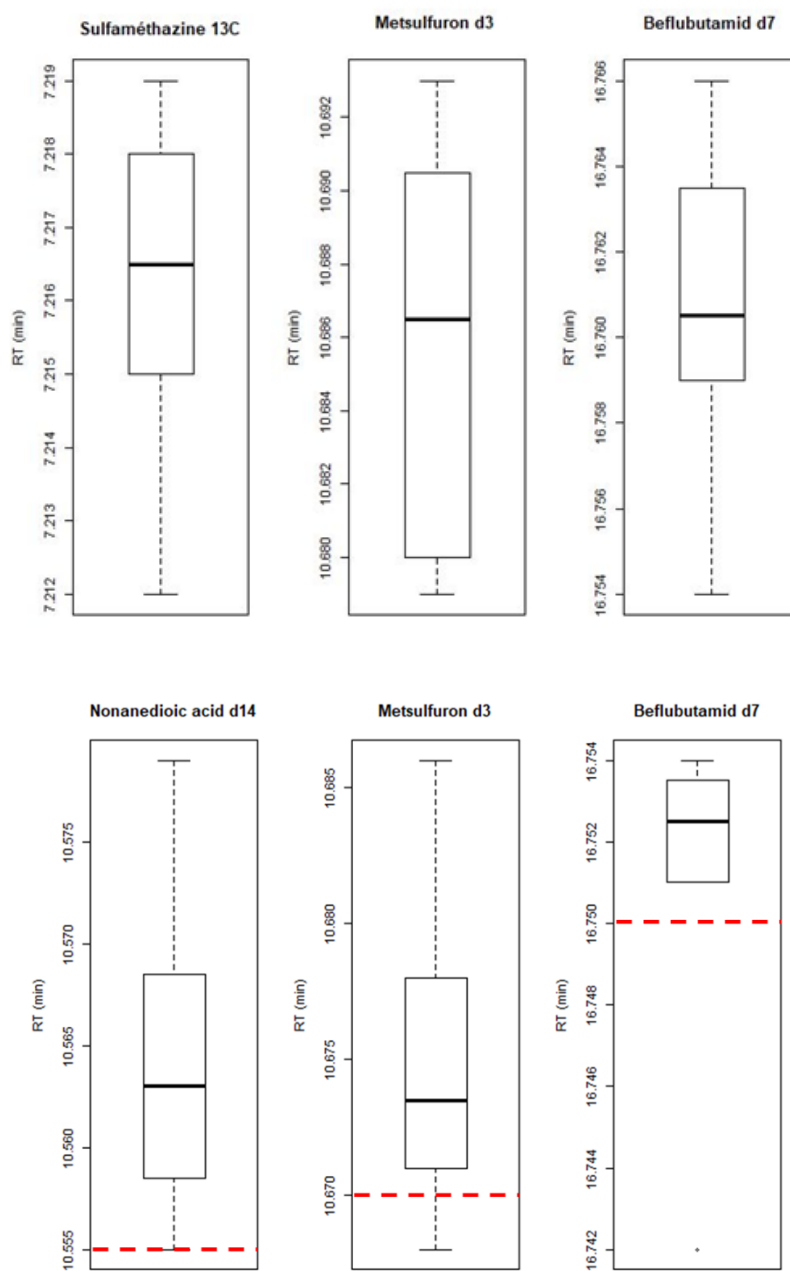
Figure S1. Variation of the monoisotopic ion retention time in QC samples of different internal standards of extraction (EIS) in ESI (+) (top) and ESI (−) (bottom) modes during sample analysis by LC-QToF. The retention time values of these compounds (corresponding to the analysis of the analytical standard for this substance) are represented by the red lines. Note they are out of the range for ^{13}C-sulfamethazine (7.425 min), metsulfuron-d_3 (16.670 min) and beflutamid-d_7 (16.750 min) in ESI (+).

65

66
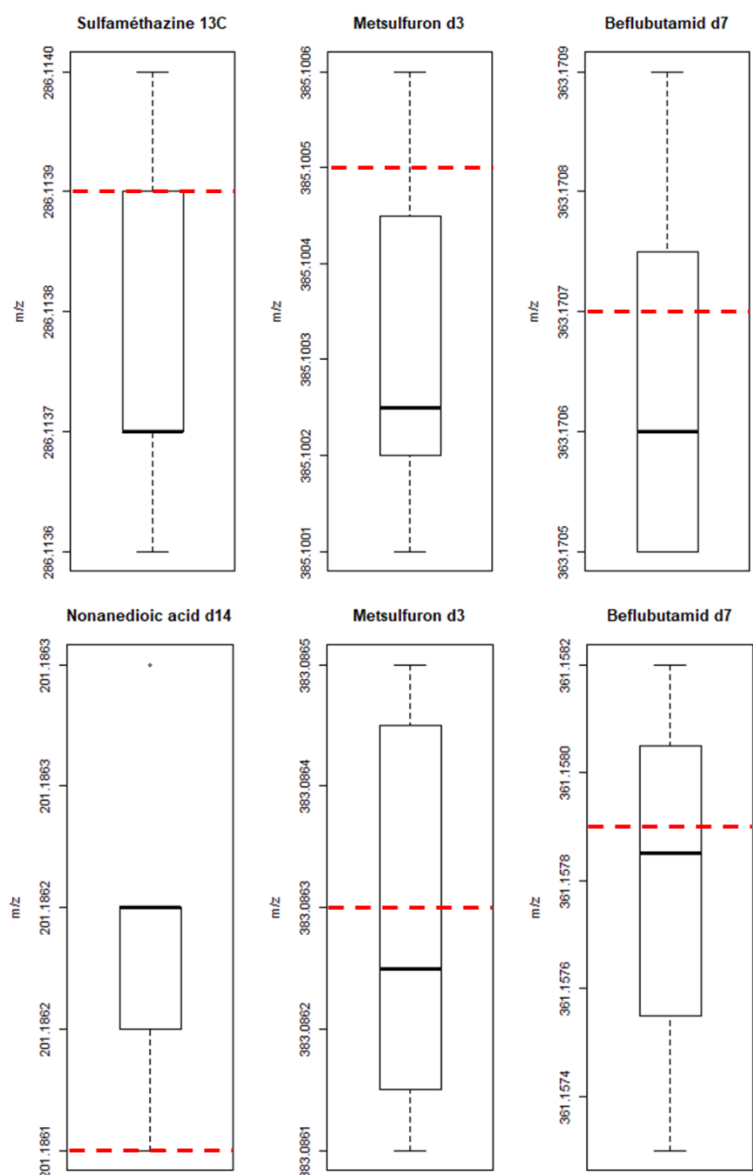
67 **Figure S2. Variation of the monoisotopic ion mass-to-charge ratio (m/z) in QC samples of different extraction internal**
68 **standards (EIS) in ESI (+) (top) and ESI (−) (bottom) mode during sample analysis by LC-QToF. The values of the**
69 **ionized molecular weights are represented by the red lines.**

70
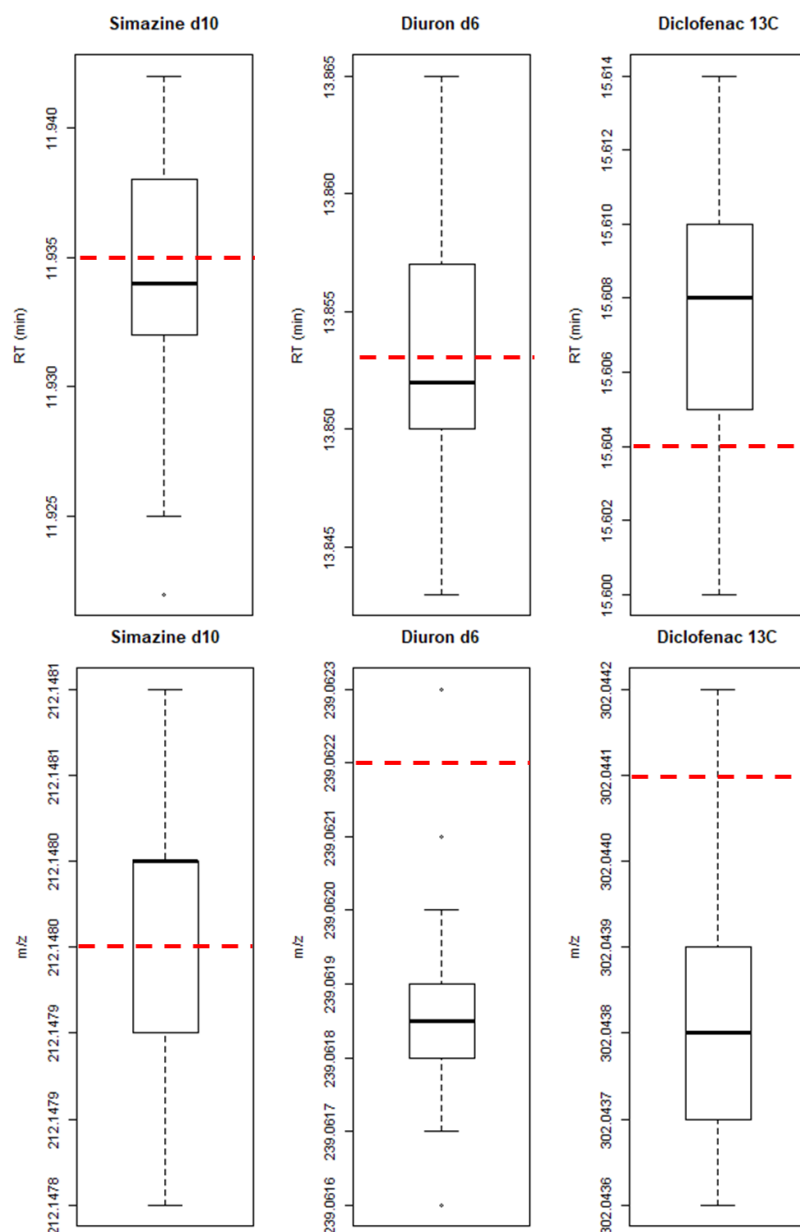
71
72 **Figure S3. Variation of the retention time (left) and the monoisotopic ion mass-to-charge ratio (m/z) (right) in QC**
73 **samples of different injection internal standards (IIS) in ESI (+) mode during sample analysis by LC-QToF. The**
74 **values of the ionized molecular weights are represented by the red lines.**

75

Figure S4. Variation of the retention time (left) and the monoisotopic ion mass-to-charge ratio (m/z) (right) in QC samples of different injection internal standards (IIS) in ESI (−) mode during sample analysis by LC-QToF. The values of the ionized molecular weights are represented by the red lines.
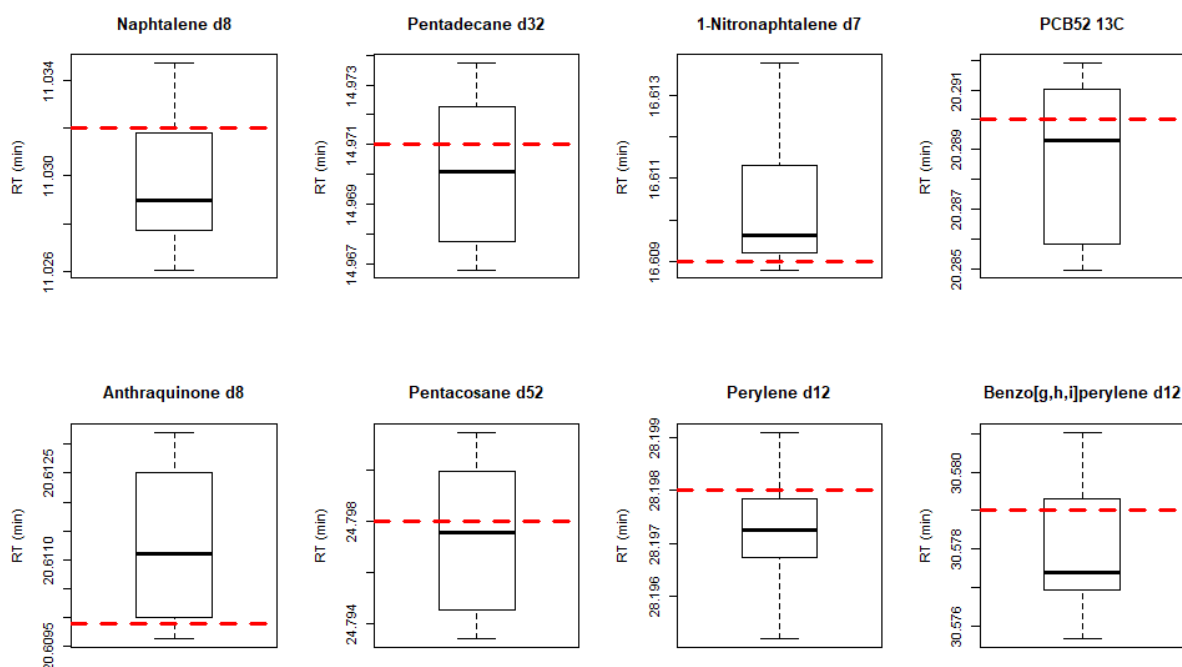
Figure S5. Variation of the retention time in QC samples of different injection internal standards (EIS) during sample analysis by GC-QToF. The values of the ionized molecular weights are represented by the red lines.
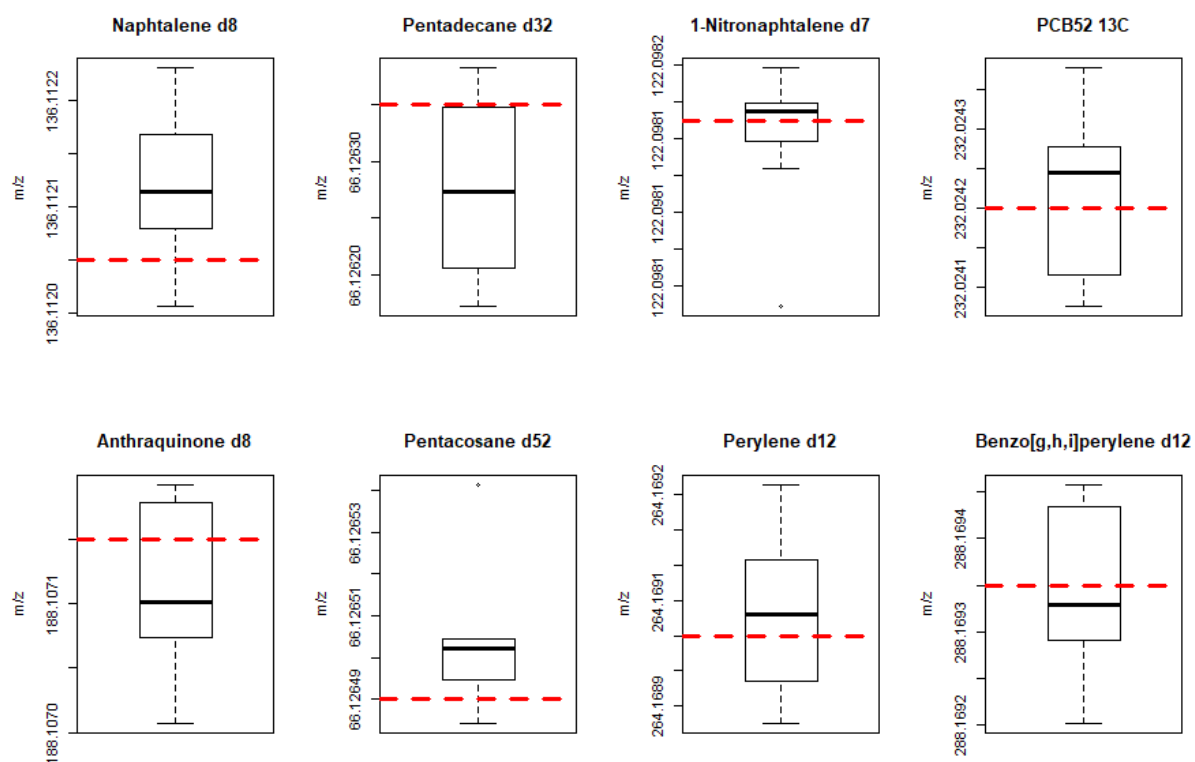
Figure S6. Variation of the monoisotopic ion mass-to-charge ratio (m/z) in QC samples of different injection internal standards (EIS) during sample analysis by GC-QToF. The values of the ionized molecular weights are represented by the red line.
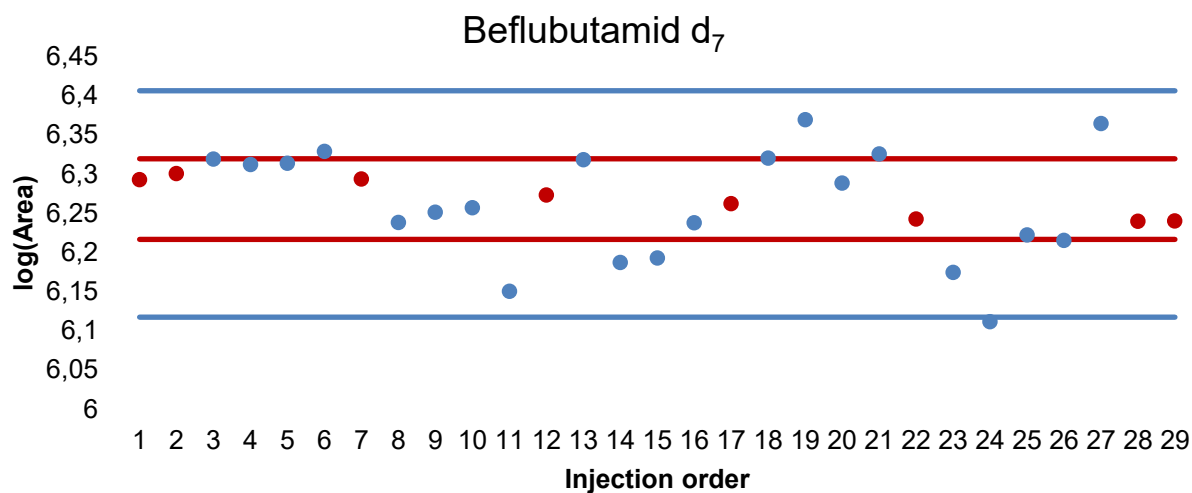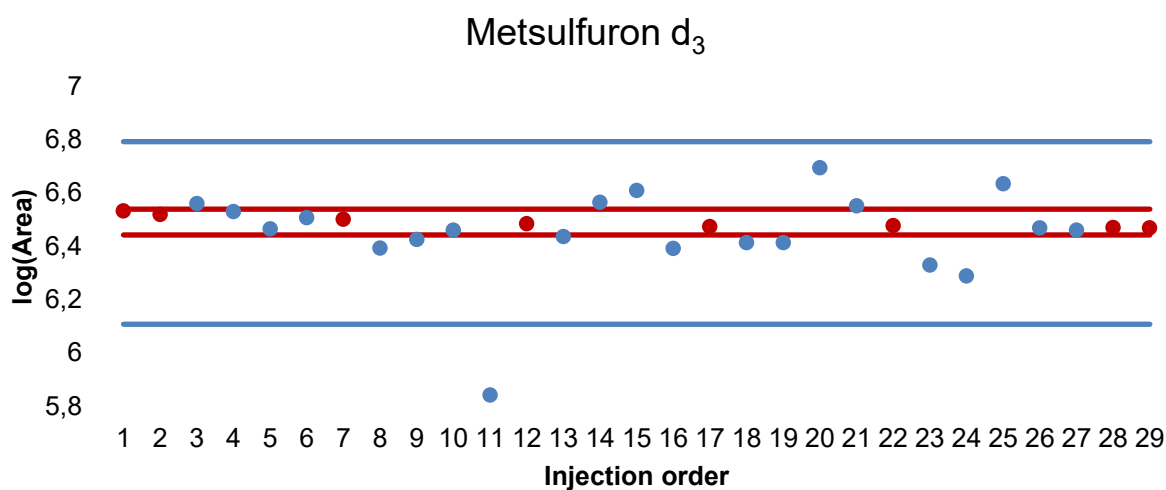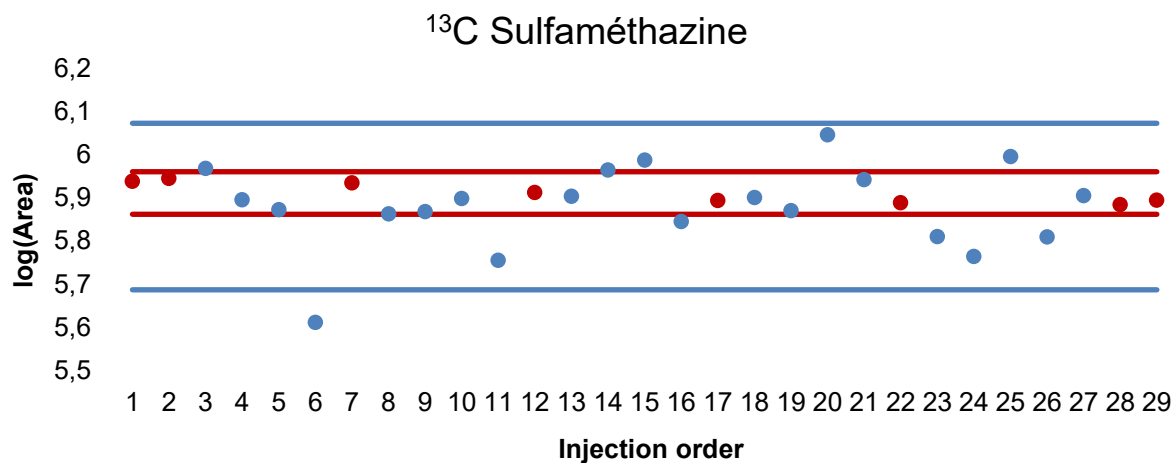
Figure S7. Control chart of areas (log area) observed for three internal extraction standards for QC pool samples (red dots) and vehicular combustion samples (blue dots) according to the injection order during LC-QToF analysis (ESI+). The red and blue lines represent the observed standard deviation (2σ) for all pooled QC and combustion samples respectively.

98
99

100
101
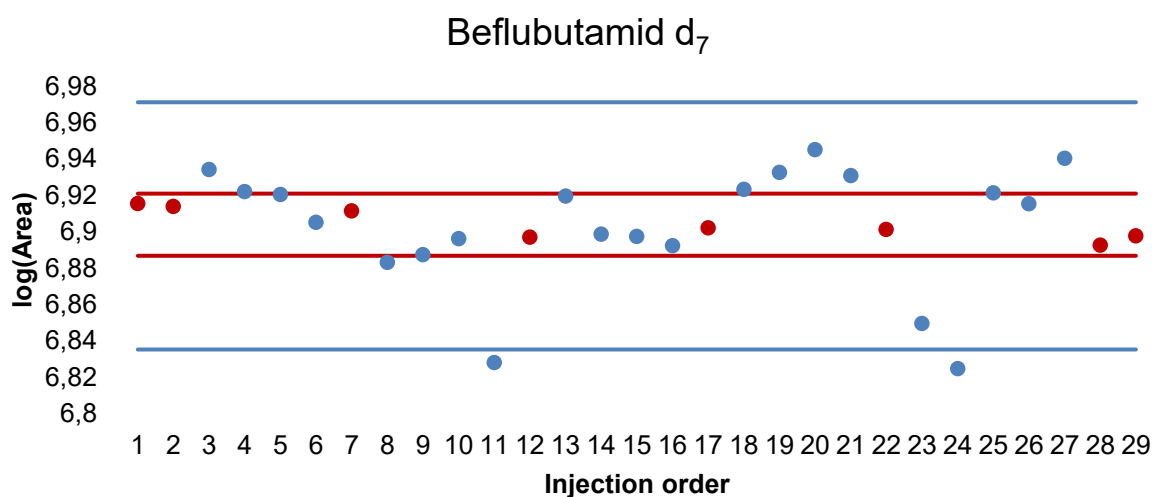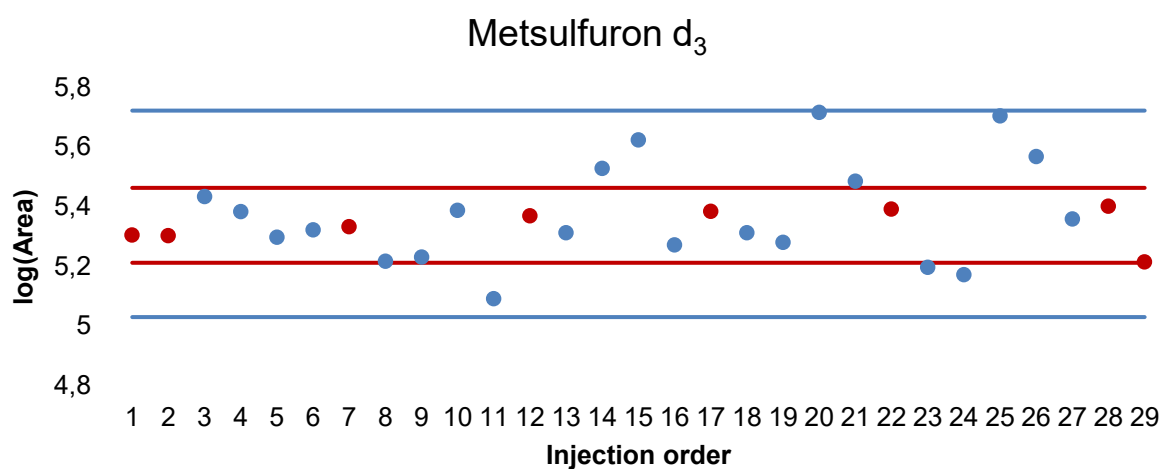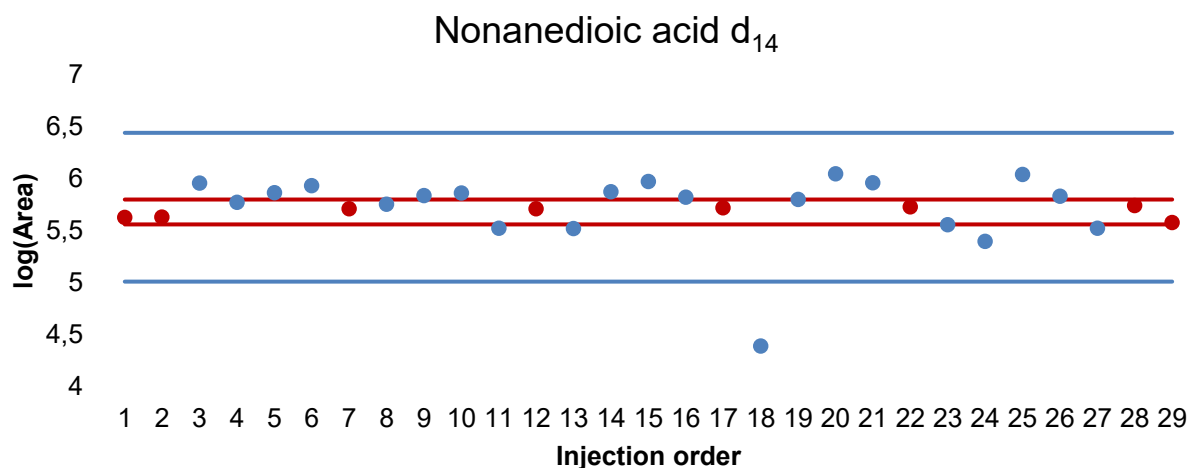
102
103 **Figure S8. Control chart of areas (log area) observed for three internal extraction standards for QC pool samples (red**
104 **dots) and vehicular combustion samples (blue dots) according to the injection order during LC-QToF analysis (ESI−).**
105 **The red and blue lines represent the observed standard deviation (2σ) for all pooled QC and combustion samples**
106 **respectively.**

107
108

109
110
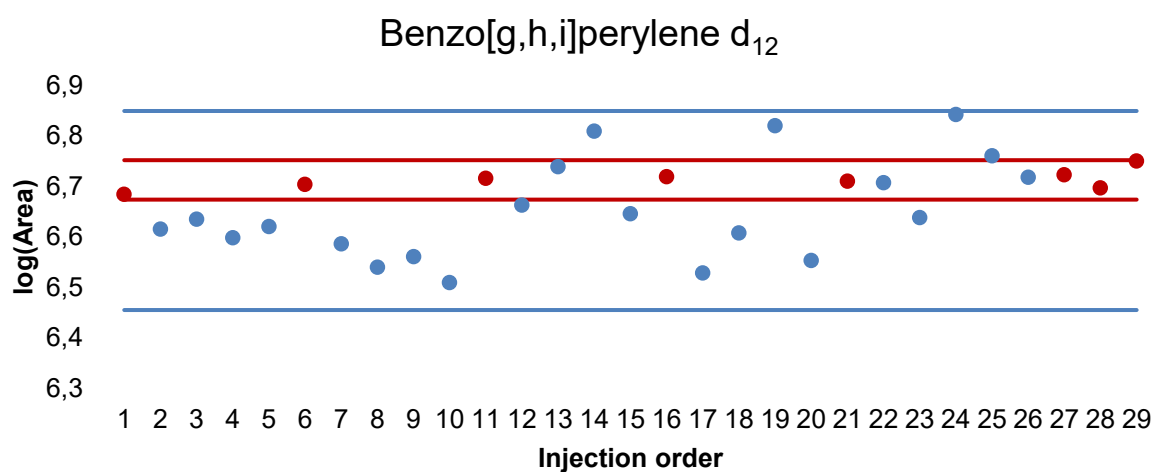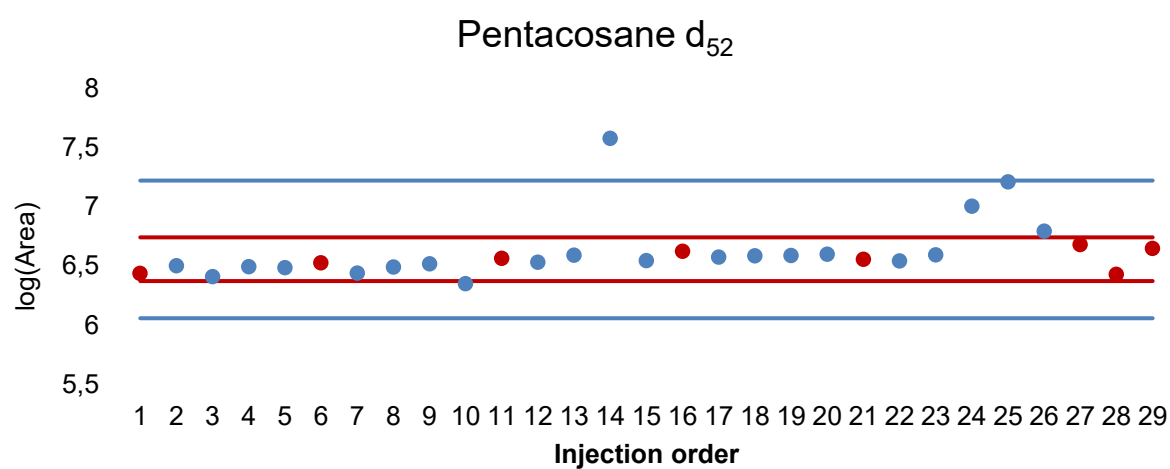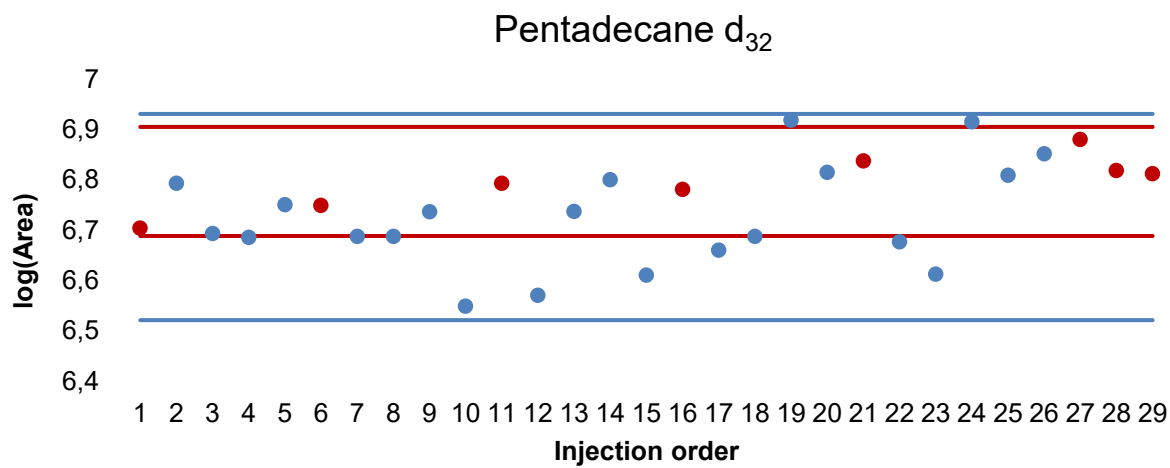
111
112 **Figure S9. Control chart of areas (log area) observed for three internal extraction standards for QC pool samples (red**
113 **dots) and vehicular combustion samples (blue dots) according to the injection order during GC-QToF analysis. The**
114 **red and blue lines represent the observed standard deviation (2σ) for all pooled QC and combustion samples**
115 **respectively.**

116

117 **5 Data treatment**

118 **Table S10. Parameters used for features extraction with the RFE algorithm (Profinder, Agilent Technologies) with the**
119 **number of detected entities and the number of entities retained in the final dataset.**

	LC-QToF		GC-QToF
	ESI (+)	ESI (−)	HEI
First step:			
- Minimal height for peaks	25000	20000	40000
- Binning and alignment:			
• Retention time window	0.15 min	0.15 min	0.05 min
• Mass window (LC)	15 ppm + 2 mDa	15 ppm + 2 mDa	/
• Dot product (GC)	/	/	0.6
- Allowed ion species adduct	H^+	H^-	
Second step:			
- Match tolerance			
• RT	± 0.15 min	± 0.15 min	± 0.05 min
• Mass	± 10 ppm	± 10 ppm	
- Minimal height for peaks	20000	12000	37000
Number of detected entities	2873	2879	2546
Number of entities in the final dataset	1833	1779	1088

120

121 **6 Overview of the particulate and gaseous emissions of EURO 5 Diesel and gasoline vehicles**

122
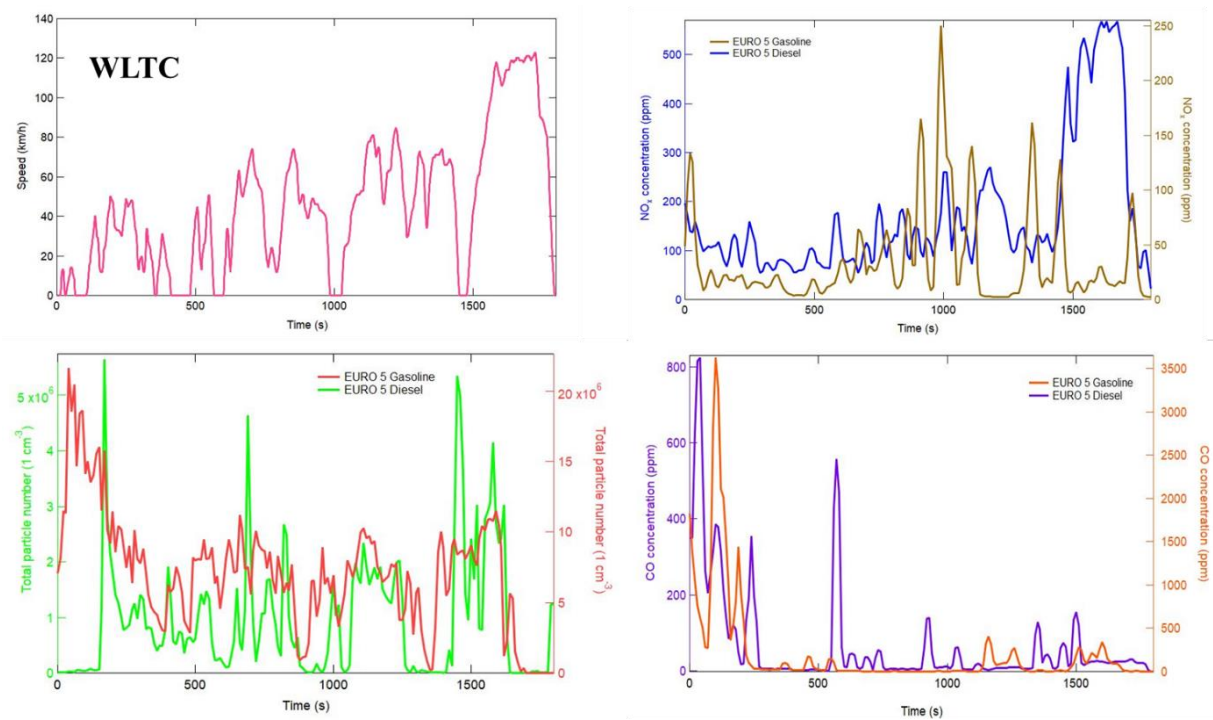
123 **Figure S10. WLTC speed profile (pink) and time series of the primary particle number measured by the CPC (bottom**
124 **left-corner), NO_x (top right-corner) and CO concentrations (bottom right-corner) at emission for the studied EURO 5**
125 **Diesel and gasoline vehicles during the ambient start WLTC driving cycle.**

126

127
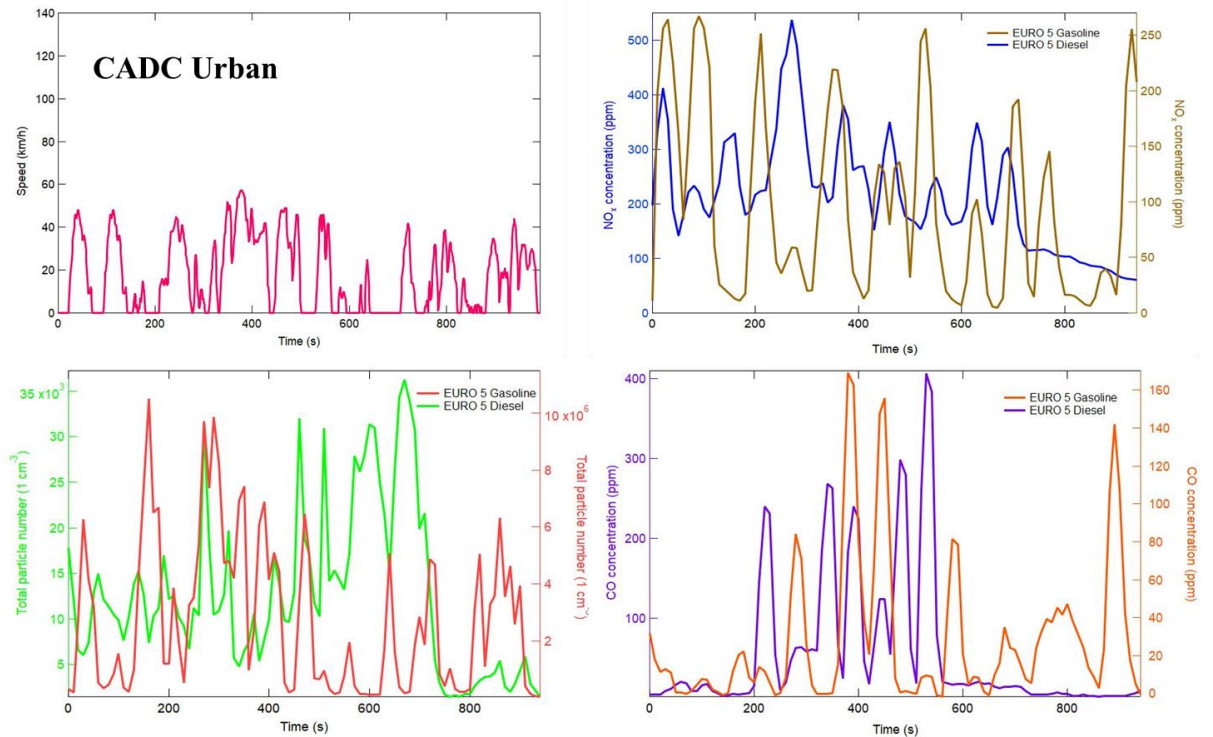
128 **Figure S11. CADC urban speed profile (pink) and time series of the primary particle number measured by the CPC**
129 **(bottom left-corner), NO_x (top right-corner) and CO concentrations (bottom right-corner) at emission for the studied**
130 **EURO 5 Diesel and gasoline vehicles during the hot-start CADC urban driving cycle.**

131
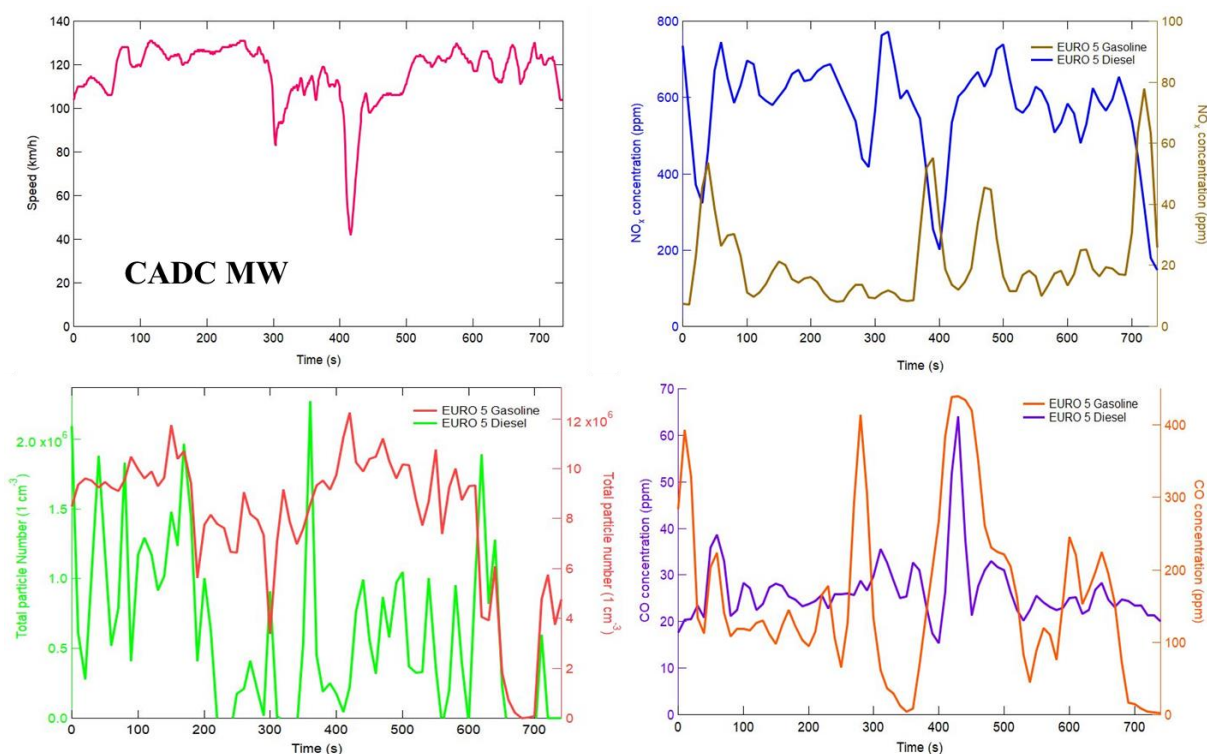
Figure S12. CADC motorway (MW) speed profile (pink) and time series of the primary particle number measured by the CPC (bottom left-corner), NOₓ (top right-corner) and CO concentrations (bottom right-corner) at emission for the studied EURO 5 Diesel and gasoline vehicles during the hot-start CADC motorway driving cycle.
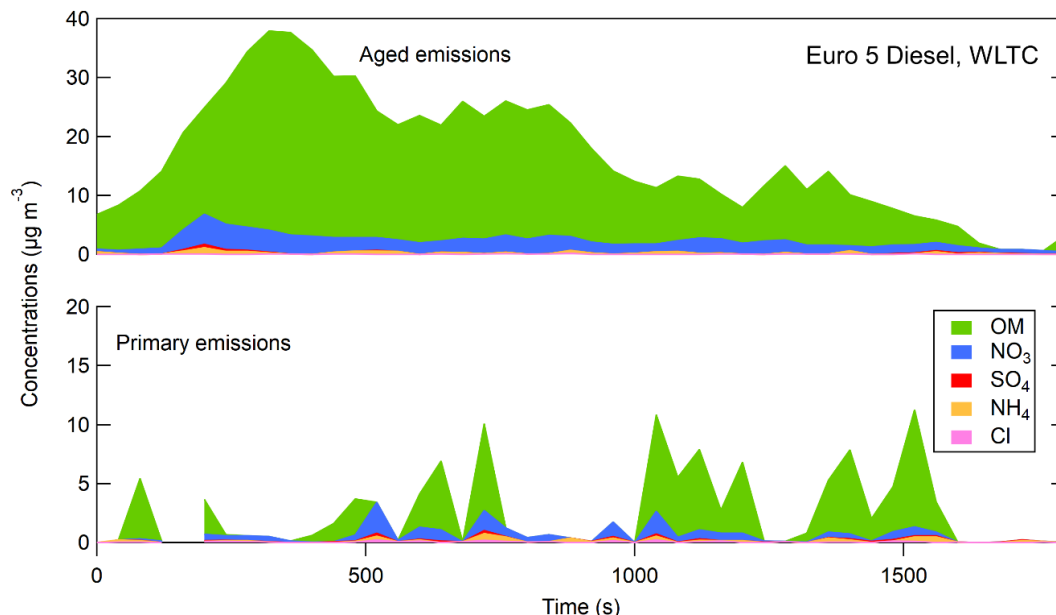
Figure S13. Temporal behaviour of organics, NO₃, SO₄, NH₄ and Cl concentrations (µg m⁻³) measured by the ACSM for the primary and aged emissions during the ambient start WLTC driving cycle for the EURO 5 Diesel vehicle. Concentrations without dilution corrections.
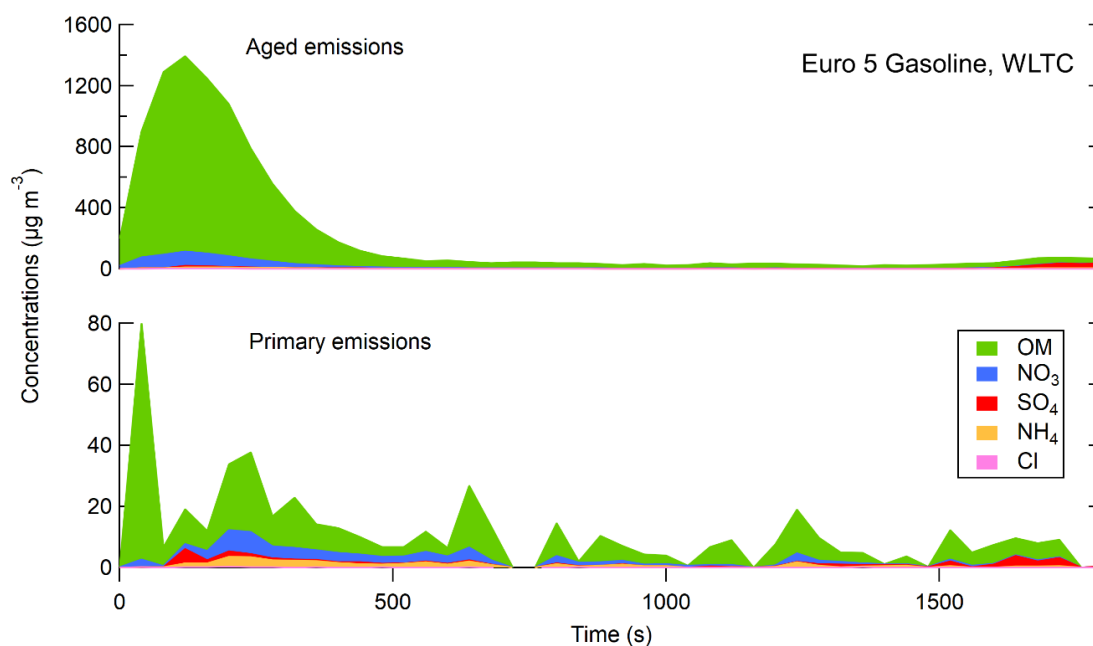
141
142 **Figure S14. Temporal behaviour of organics, NO₃, SO₄, NH₄ and Cl concentrations (μg m⁻³) measured by the ACSM**
143 **for the primary and aged emissions during the ambient start WLTC driving cycle for the EURO 5 gasoline vehicle.**
144 **Concentrations without dilution corrections.**
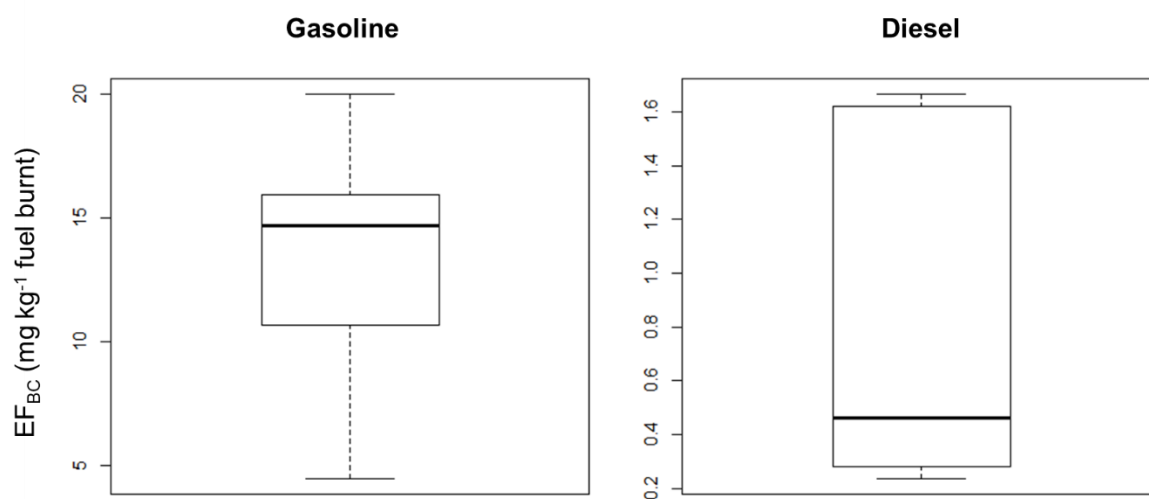
145
146 **Figure S15. Boxplot of the primary BC concentrations (μg m⁻³) obtained for the EURO 5 gasoline and Diesel vehicles**
147 **(all driving cycles).**

148

149 **7 Non-target chemical characterization of vehicular OA.**

150

151
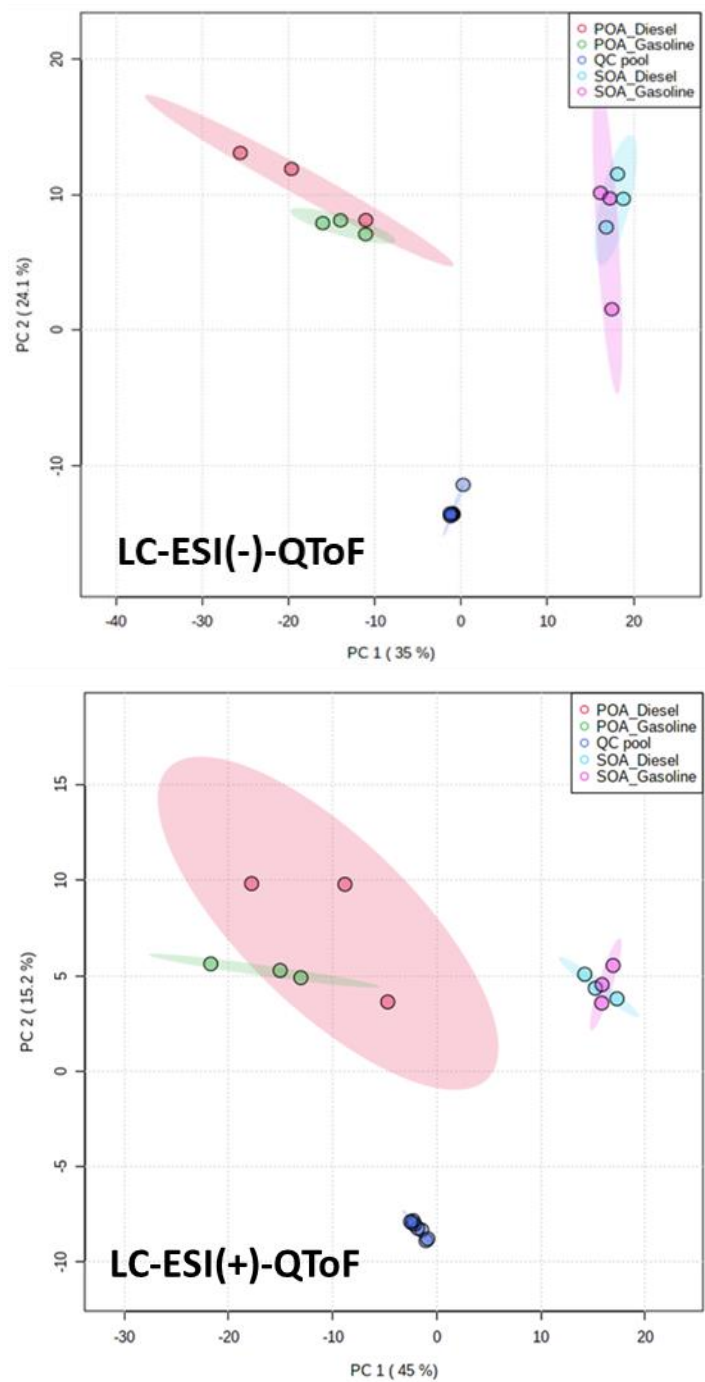
152 **Figure S16. Principal component analysis of samples from primary and secondary vehicular emissions (POA Diesel:**
153 **red, POA gasoline: green, SOA Diesel: light blue, SOA gasoline: pink) and pooled QC samples (dark blue). The result**
154 **is obtained from the NTS analysis performed by LC-QToF (ESI(+) and ESI(−) mode). The data were normalized by**
155 **pooled QC samples, log-transformed and auto-scaled. The ellipses represent the 95 % confidence zones.**

156
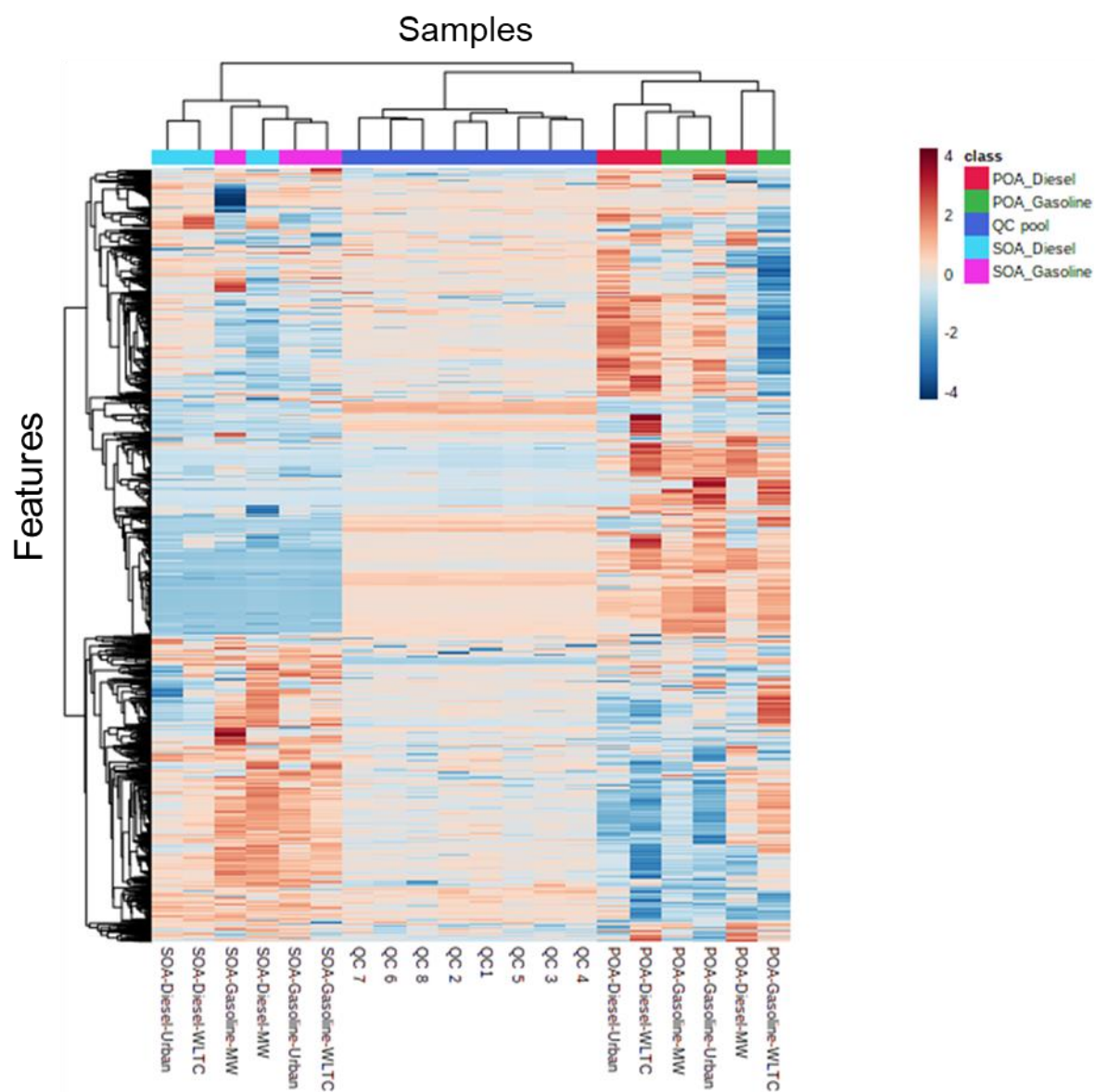
Figure S17. Two-way hierarchical classification and heat map of the different vehicular exhaust samples from LC-QToF analysis in ESI(+) mode. This classification was performed based on the Pearson correlation coefficient using the average linkage method. The colour-scale on the right represented the feature relative abundance in each sample compared to the others.

161
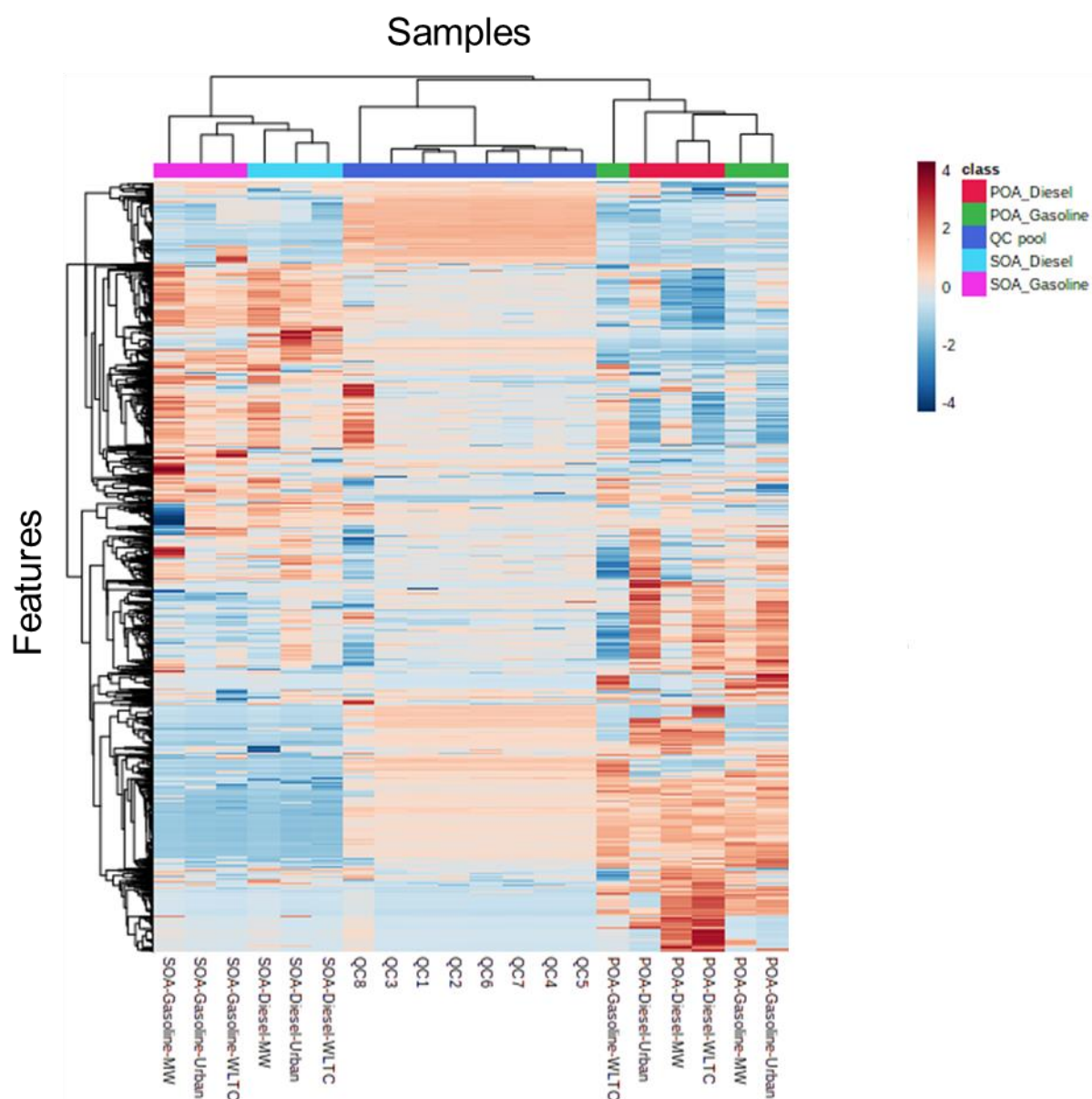
Figure S18. Two-way hierarchical classification and heat map of the different vehicular exhaust samples from LC-QToF analysis in ESI(−) mode. This classification was performed based on the Pearson correlation coefficient using the average linkage method. The colour-scale on the right represented the feature relative abundance in each sample compared to the others.

166

167

168

169

170

171

172
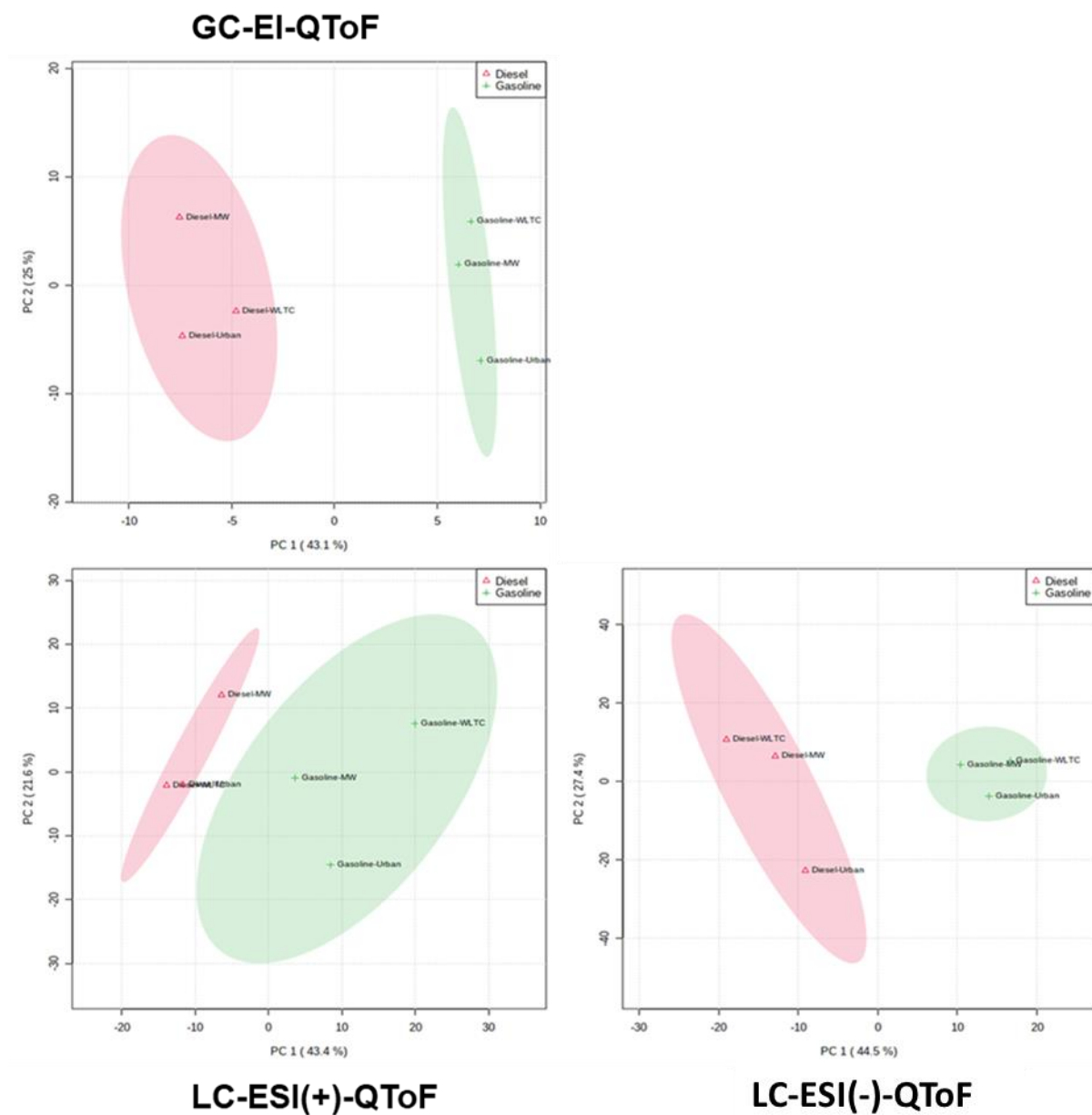
Figure S19. Principal component analyses (PCA) of POA samples from gasoline (green) and Diesel (red) vehicles. The
results are obtained from the GC-QToF and LC-QToF data and were normalized by pooled QC samples, log-
transformed and auto-scaled. The ellipses represent the 95 % confidence zones.

176
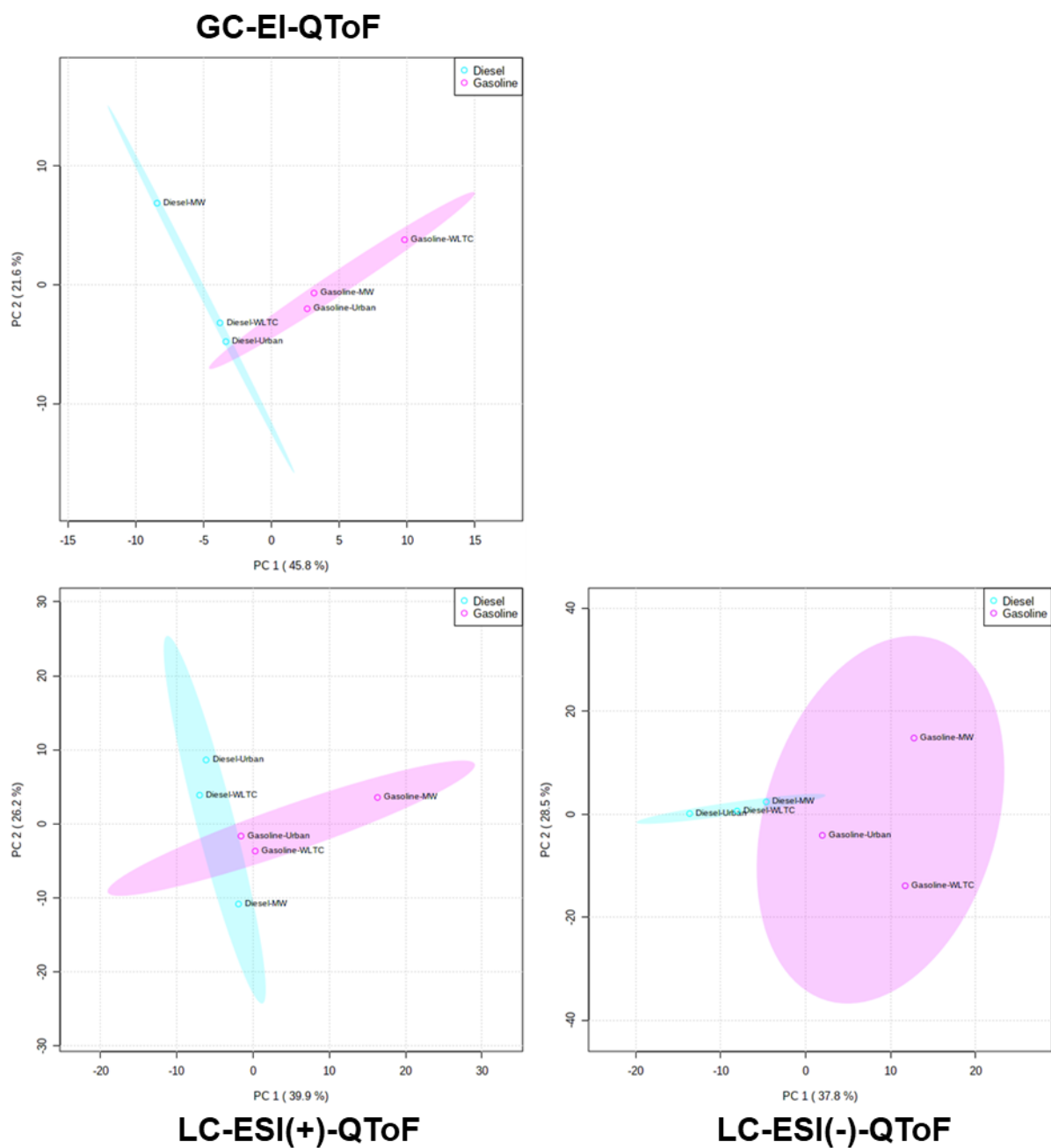
Figure S20. Principal component analyses (PCA) of SOA samples from gasoline (pink) and Diesel (light blue) vehicles. The results are obtained from the GC-QToF and LC-QToF data and were normalized by pooled QC samples, log-transformed and auto-scaled. The ellipses represent the 95 % confidence zones.

183   **Table S11. Predictive ability of the different PLS-DA models**

OA fraction	Analysis	R²X	Q²X
POA	GC-QToF	0.99	0.83
	LC-ESI(+)-QToF	0.97	0.65
	LC-ESI(−)-QToF	0.98	0.70
SOA	GC-QToF	0.99	0.83
	LC-ESI(+)-QToF	1.00	0.30
	LC-ESI(−)-QToF	0.98	0.50

184

185

186
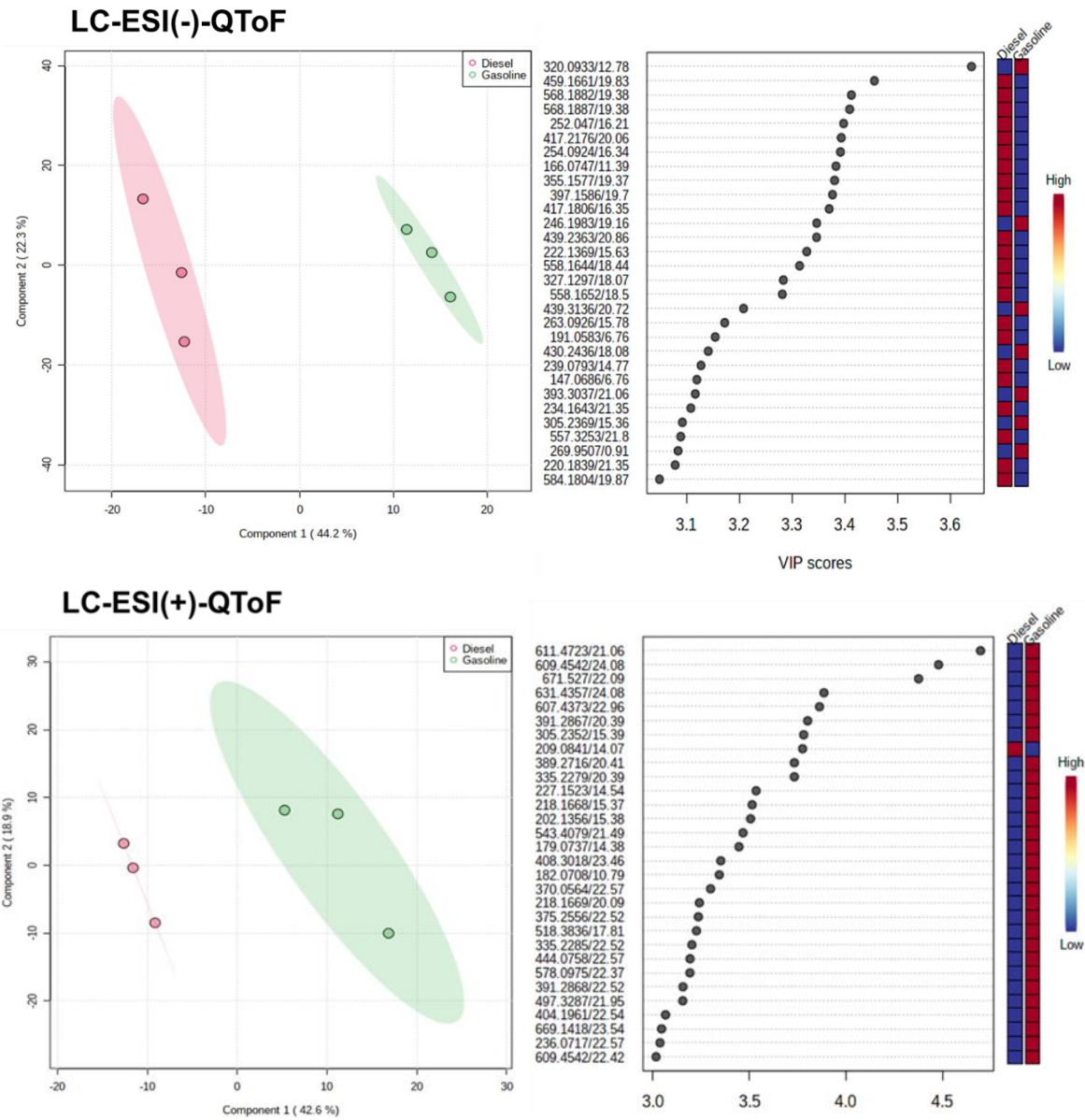
187   **Figure S21. Partial Least Square–Discriminant Analysis (PLS-DA) of POA samples from gasoline and Diesel vehicles.**
188   **The results are obtained from the GC-QToF and LC-QToF (both positive and negative mode) data and were**
189   **normalized by pooled QC samples, log-transformed and auto-scaled. The ellipses represent the 95 % confidence**
190   **zones. Classification of chemical entities (left scale: molecular mass/retention time) characteristic of each vehicular**
191   **source according to the VIP score are displayed on the right. The colour scale indicates the variation in abundance of**
192   **the chemical entity (100 % = red, 0 % = blue) in all samples of both vehicles. Only the first 30 chemical entities with**
193   **the highest VIP scores are shown on the graph.**

194

195

196
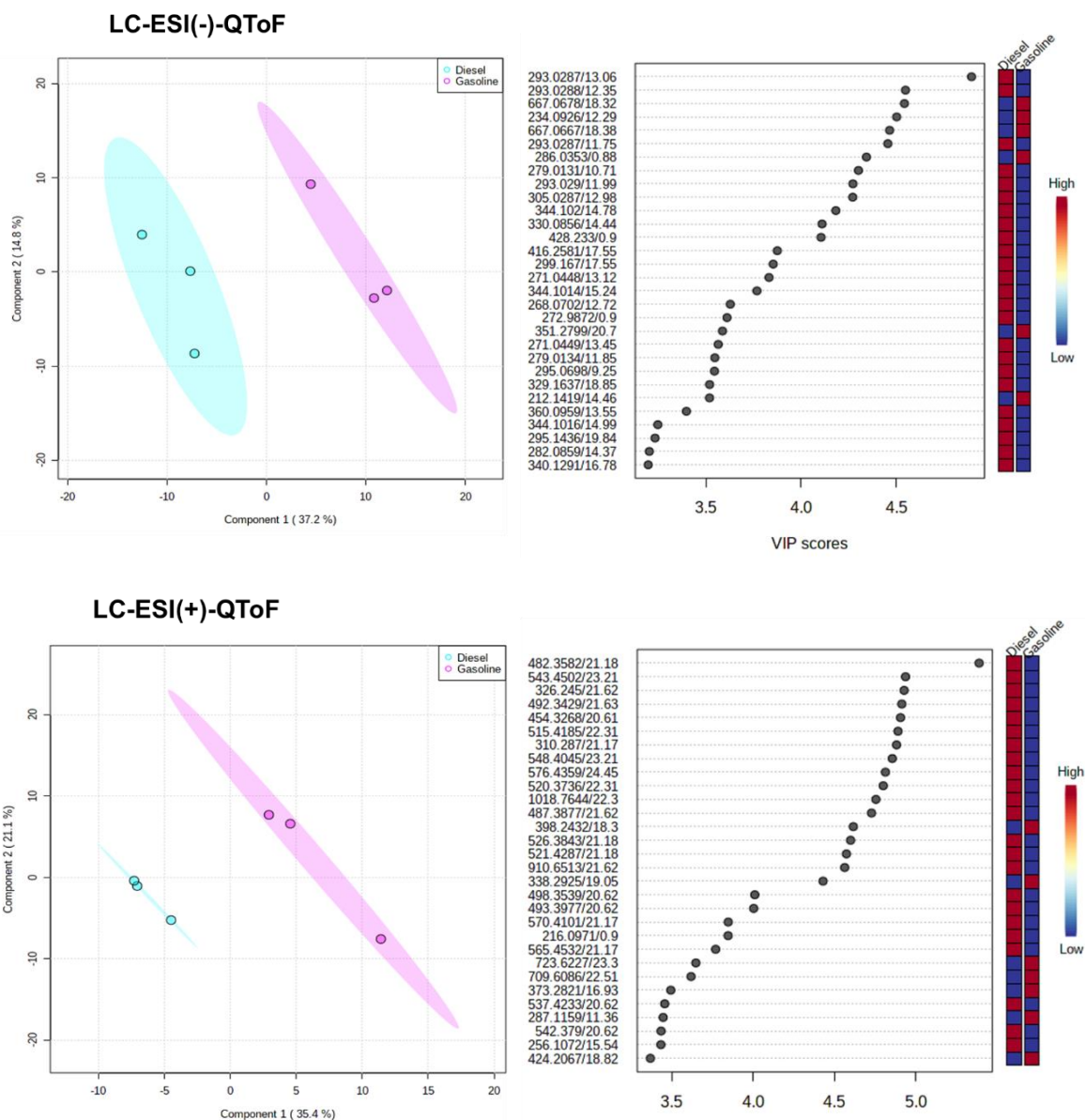
197 **Figure S22. Partial Least Square–Discriminant Analysis (PLS-DA) of SOA samples from gasoline and Diesel vehicles.**
198 **The results are obtained from the GC-QToF and LC-QToF (positive and negative mode) data and were normalized**
199 **by pooled QC samples, log-transformed and auto-scaled. The ellipses represent the 95 % confidence zones.**
200 **Classification of chemical entities (left scale: molecular mass /retention time for LC) characteristic of each vehicular**
201 **source according to the VIP score are displayed on the right. The colour scale indicates the variation in abundance of**
202 **the chemical entity (100 % = red, 0 % = blue) in all samples of both vehicles. Only the first 30 chemical entities with**
203 **the highest VIP scores are shown on the graph.**

8 Tentative identifications of POA and SOA markers

Table S12. Selected markers (molecular mass or base peak, Da/retention time, min) and their tentative identification. Questionable molecular formulas are highlighted in yellow (see 3.3 in the main text).

POA Diesel			POA Gasoline			SOA Diesel			SOA Gasoline		
GC-QToF											
GC POA D-1	68.0256/7.57	2H-Pyran-2-one	GC POA G-1	208.0885/21.02	-	GC SOA D-1	101.0597/16.16	-	GC SOA G-1	127.0750/8.49	-
									GC SOA G-2	129.0909/11.56	-
LC-QToF (ESI negative mode)											
LC NEG POA D-1	254.0924/16.34	$C_9H_{23}CoO_4$ $C_8H_{16}CaN_5O_2$ $C_{10}H_{18}Al_2NO_3$	LC NEG POA G-1	320.0933/12.78	$C_7H_{27}MnNO_7Si$ $C_8H_{26}Al_4NO_3Si$	LC NEG SOA D-1	271.0499/13.45	$C_8H_{13}Al_2N_2O_5$ $C_5H_{16}CoN_4O_5$	LC NEG SOA G-1	234.0926/12.29	$C_7H_{20}Al_2N_2OS$ $C_{10}H_{18}O_4S$
LC NEG POA D-2	327.1297/18.07	$C_{16}H_{24}Al_3NO$ $C_{12}H_{13}N_{11}O$				LC NEG SOA D-2	279.0131/10.71	$C_9H_9Al_2N_2O_5$ $C_{12}H_7O_8$			
LC NEG POA D-3	355.1577/19.37	$C_{17}H_{22}AlN_5O_2$ $C_{20}H_{28}CoN_2$				LC NEG SOA D-3	293.0287/13.06	$C_{10}H_{11}Al_2N_2O_5$ $C_{11}H_7N_3O_7$			
LC NEG POA D-4	397.1586/19.70	$C_{19}H_{28}Al_3N_2O_2$ $C_{19}H_{32}CaMnN_3$				LC NEG SOA D-4	293.0290/11.99	$C_{13}H_9O_8$ $C_{11}H_7N_3O_7$			
LC NEG POA D-5	417.1806/16.35	$C_{15}H_{28}AlN_5O_7$				LC NEG SOA D-5	305.0287/12.98	$C_{14}H_9O_8$			
LC NEG POA D-6	459.1661/19.83	$C_{21}H_{29}Al_2N_2O_6$ $C_{20}H_{23}Al_2N_9O$				LC NEG SOA D-6	330.0856/14.44	$C_{16}H_{14}N_2O_6$ $C_{15}H_{18}Al_2NO_4$			
LC NEG POA D-7	568.1882/19.38	$C_{31}H_{32}Al_4N_4$ $C_{27}H_{32}Al_2CaN_4O$				LC NEG SOA D-7	344.1020/14.78	$C_{18}H_{12}N_6O_2$ $C_{14}H_{18}Al_2N_4O_4$			
LC NEG POA D-8	584.1804/19.87	$C_{25}H_{41}AlCoN$ $C_{28}H_{43}AlCo_2N_2O_2$				LC NEG SOA D-8	360.0959/13.55	$C_{18}H_{12}N_6O_3$ $C_{12}H_{32}Mn_2NO_2Si$			
LC-QToF (ESI positive mode)											
LC POS POA D-1	209.0841/14.07	$C_{14}H_{11}NO$ $C_{12}H_9N_4$ $C_8H_{15}MnN_3O$	LC POS POA G-1	202.1356/15.39	$C_{12}H_{16}N_3$ $C_{14}H_{18}O$	LC POS SOA D-1	576.4359/24.45	$C_{30}H_{60}N_2O_8$	LC POS SOA G-1	287.1156/11.36	$C_{16}H_{17}NO_4$ $C_{14}H_{15}N_4O_3$
			LC POS POA G-2	305.2352/15.39	$C_{17}H_{29}N_4O$ $C_{19}H_{31}NO_2$ $C_{12}H_{36}MnN_5$	LC POS SOA D-2	1018.7644/22.30	N.A.			
			LC POS POA G-3	335.2279/20.39	$C_{23}H_{29}NO$ $C_{21}H_{27}N_4$						
			LC POS POA G-4	375.2556/22.52	$C_{24}H_{31}N_4$ $C_{26}H_{33}NO$						
			LC POS POA G-5	389.2716/20.41	$C_{25}H_{33}N_4$ $C_{22}H_{42}MnN_2$ $C_{27}H_{35}NO$						
			LC POS POA G-6	391.2867/20.39	$C_{25}H_{35}N_4$ $C_{27}H_{37}NO$						
			LC POS POA G-7	543.4079/21.49	$C_{37}H_{53}NO_2$ $C_{35}H_{51}N_4O$						
			LC POS POA G-8	607.4373/22.96	$C_{42}H_{57}NO_2$						
			LC POS POA G-9	609.4542/24.08	$C_{40}H_{57}N_4O$ $C_{42}H_{59}NO_2$						
			LC POS POA G-10	611.4723/21.06	$C_{34}H_{74}Al_2CoO$ $C_{42}H_{61}NO_2$						
			LC POS POA G-11	671.5270/22.09	$C_{45}H_{69}NO_3$ $C_{42}H_{71}Al_2N_3$						

8   Some examples of chromatographic responses of markers.
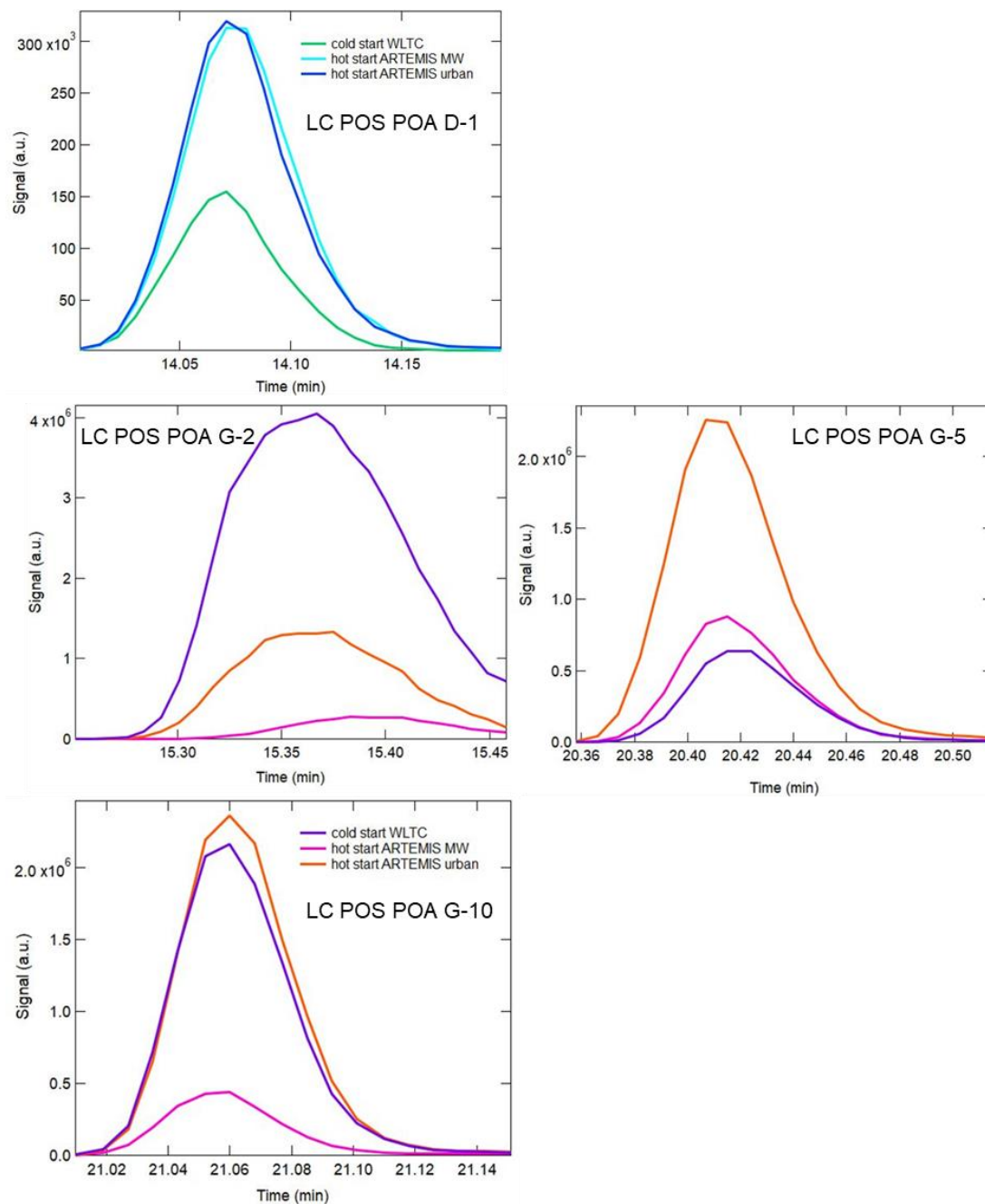
Figure S23. Potential molecular markers characteristic of Diesel and gasoline POA from LC-QToF data in positive mode (ESI+).
Chromatographic response observed for selected markers in ambient start WLTC, hot-start CADC motorway (MW) and urban
driving conditions.
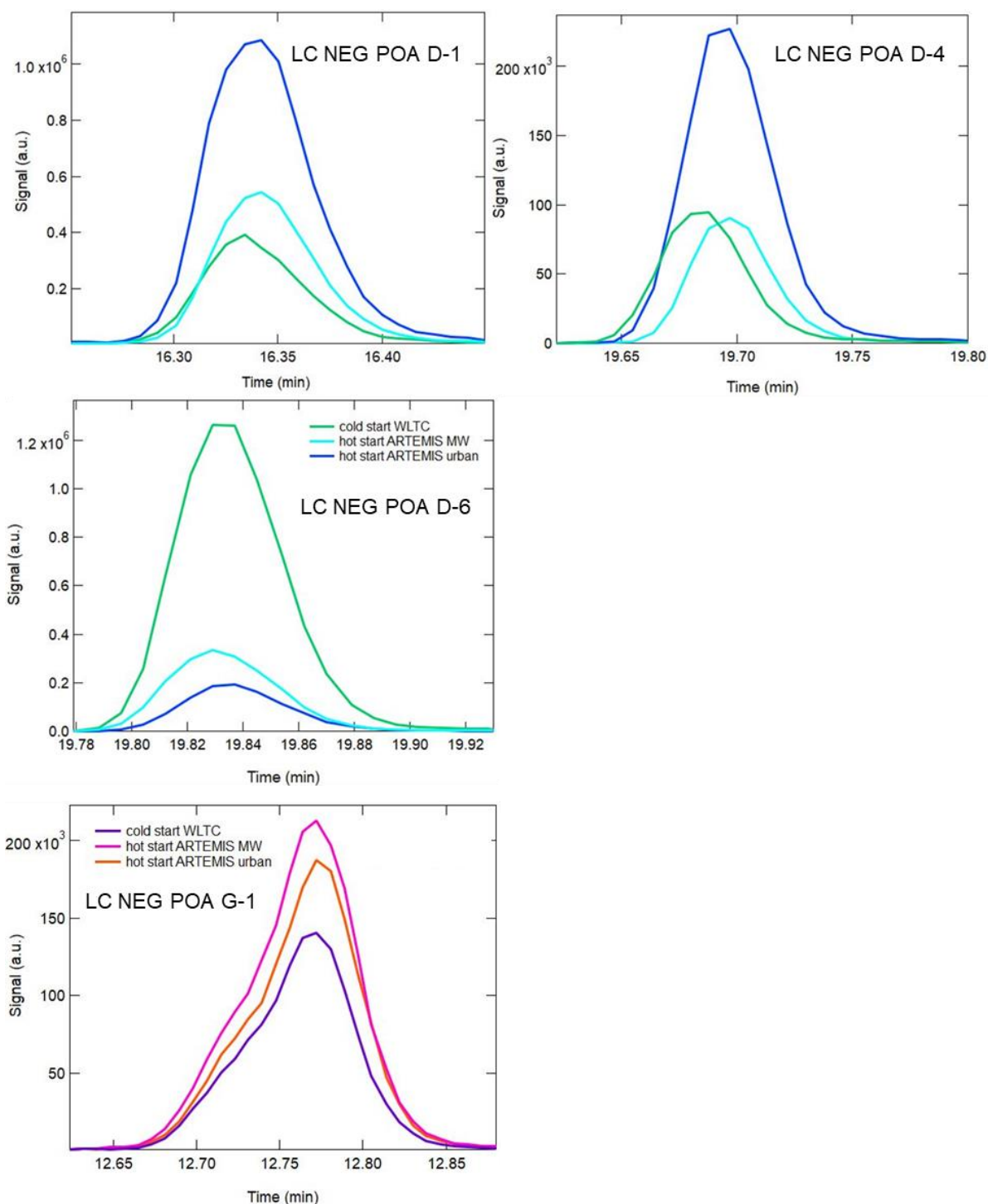
Figure S24. Potential molecular markers characteristic of Diesel and gasoline POA from LC-QToF data in negative mode (ESI−). Chromatographic response observed for selected markers in ambient start WLTC, hot-start CADC motorway (MW) and urban driving conditions.
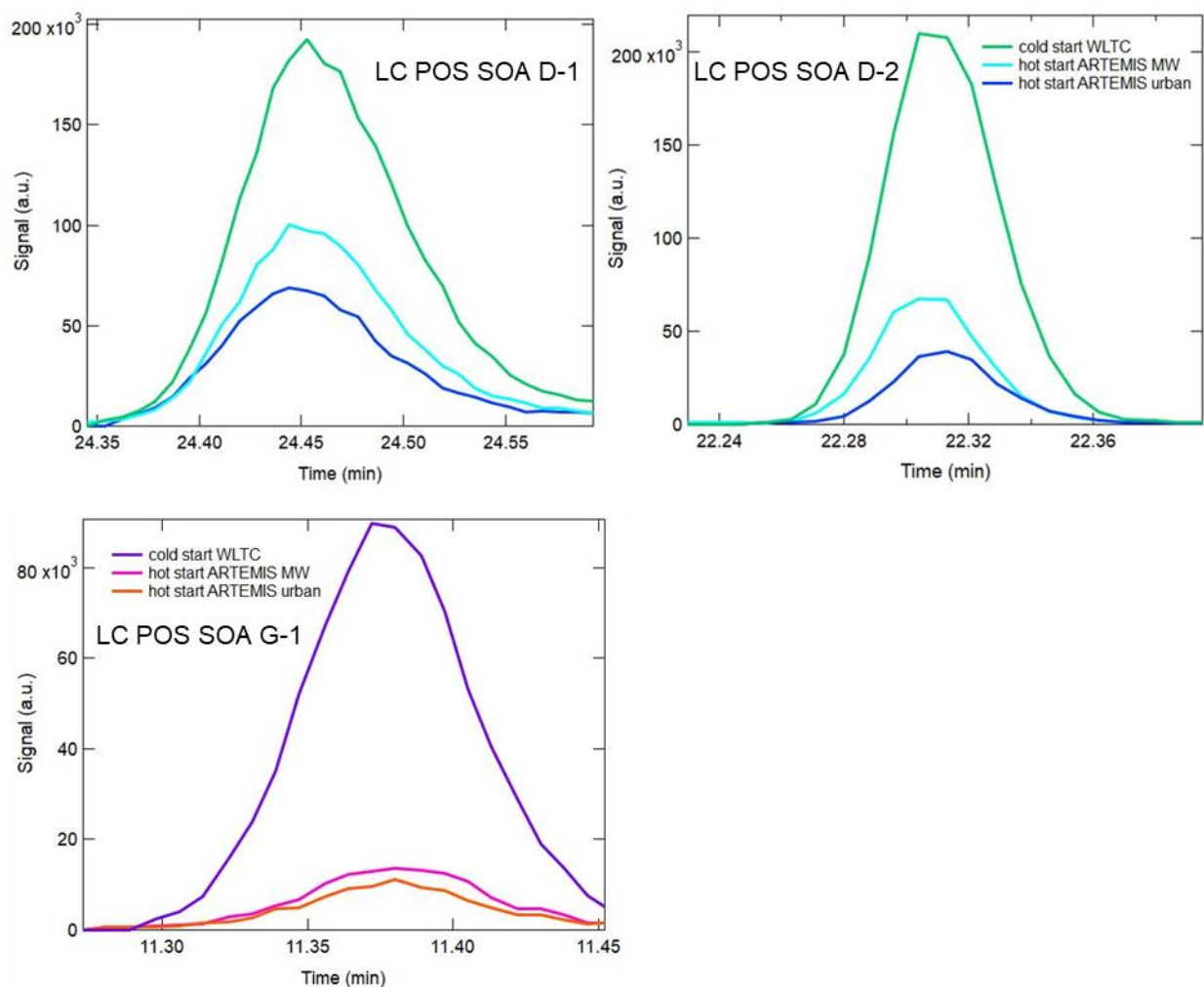
Figure S25. Potential molecular markers characteristic of Diesel and gasoline SOA from LC-QToF data in positive mode (ESI+). Chromatographic response observed for selected markers in ambient start WLTC, hot-start CADC motorway (MW) and urban driving conditions.
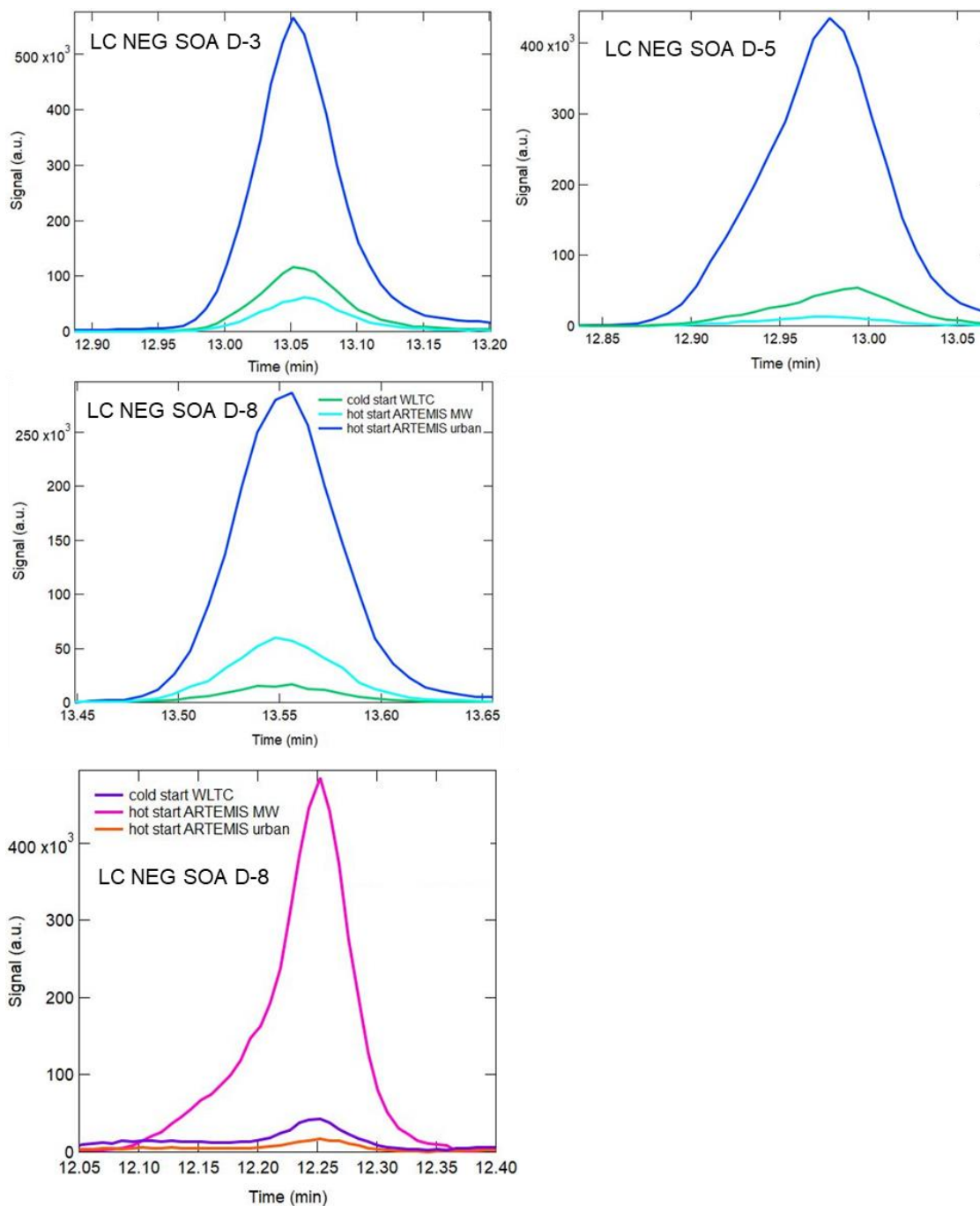
Figure S26. Potential molecular markers characteristic of Diesel and gasoline SOA from LC-QToF data in negative mode (ESI−). Chromatographic response observed for selected markers in ambient start WLTC, hot-start CADC motorway (MW) and urban driving conditions.
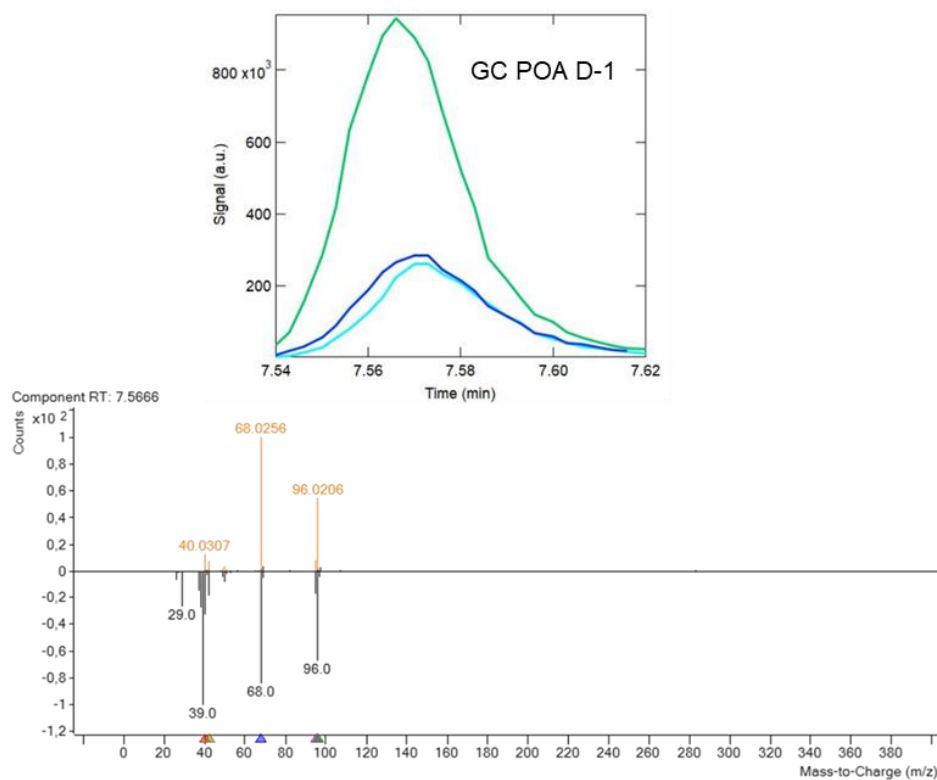
Figure S27. Chromatographic response of the feature base peak (m/z = 68.0256) and head-to-tail EI mass spectra of the POA Diesel marker GC-POA D-1 and the 2H-pyran-2-one from GC-QToF data (acquisition started at 40 m/z).
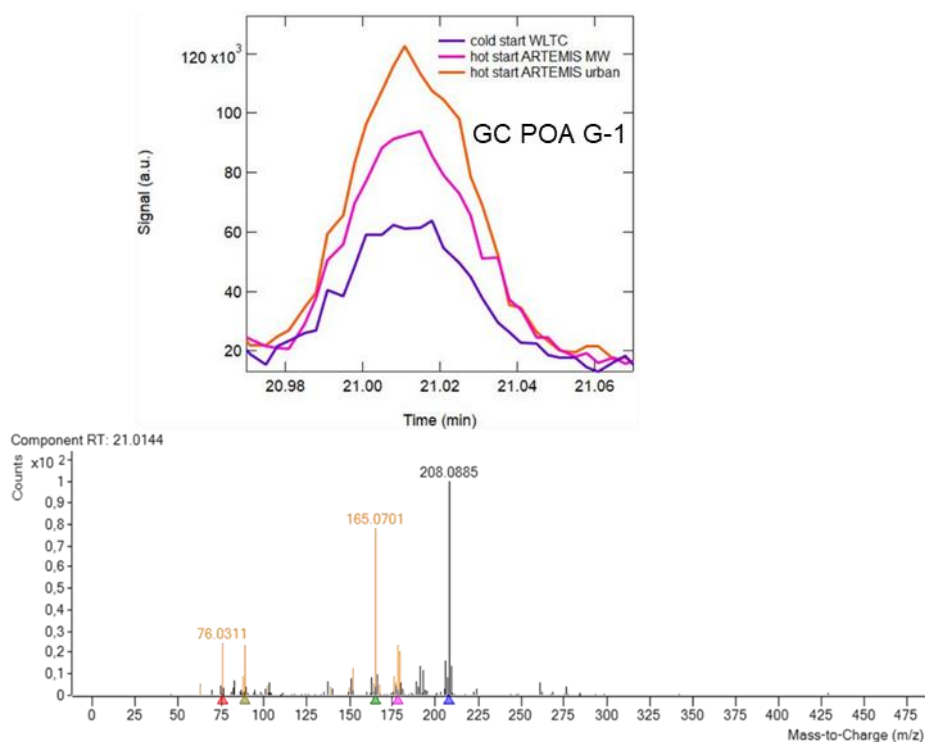
Figure S28. Chromatographic response of the feature base peak (m/z = 208.0885) and the EI mass spectra of the POA gasoline marker GC POA G-1 from GC-QToF data (acquisition started at 40 m/z).
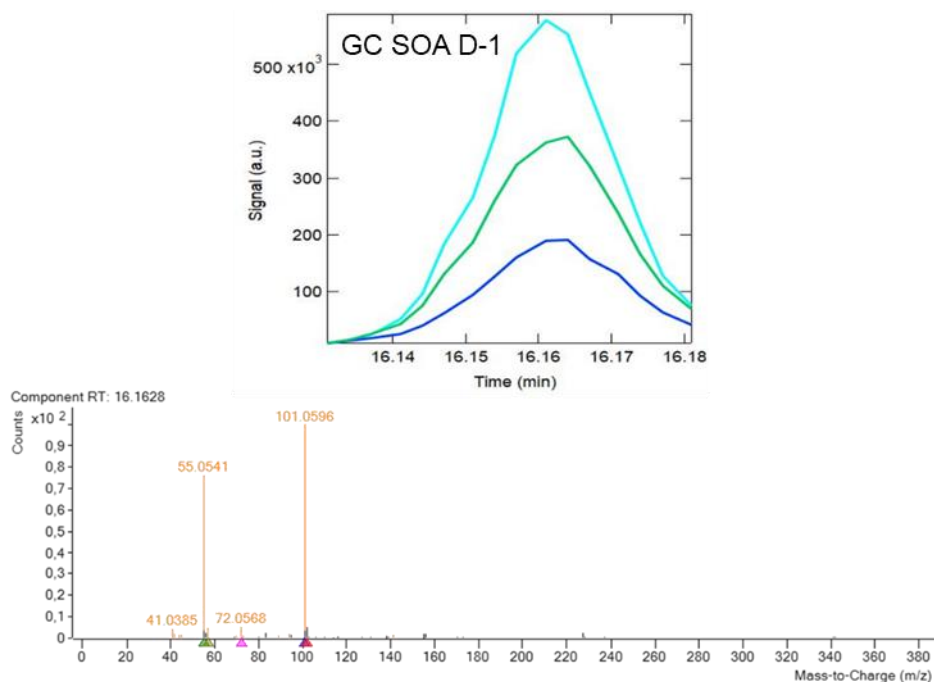
35   **Figure S29. Chromatographic response of the feature base peak (m/z = 101.0597) and the EI mass spectra of the SOA Diesel marker GC SOA D-1 from GC-QToF data (acquisition started at 40 m/z).**
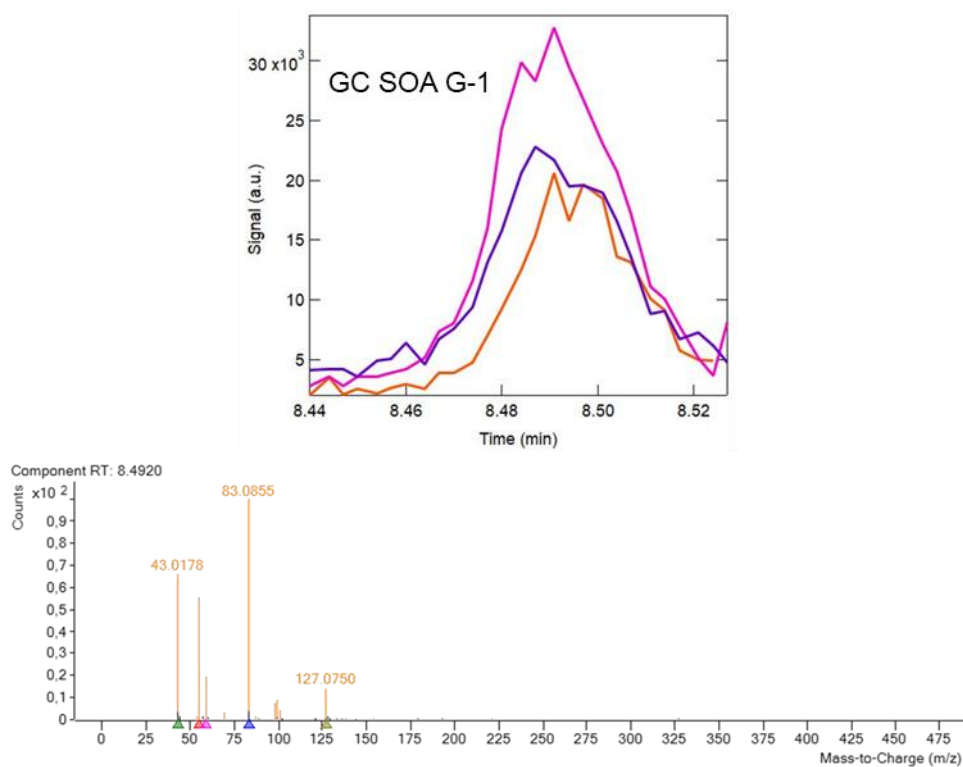
Figure S30. Chromatographic response of the feature base peak (m/z = 127.0750) and the EI mass spectra of for one SOA gasoline marker GC SOA G-1 from GC-QToF data (acquisition started at 40 m/z).

40
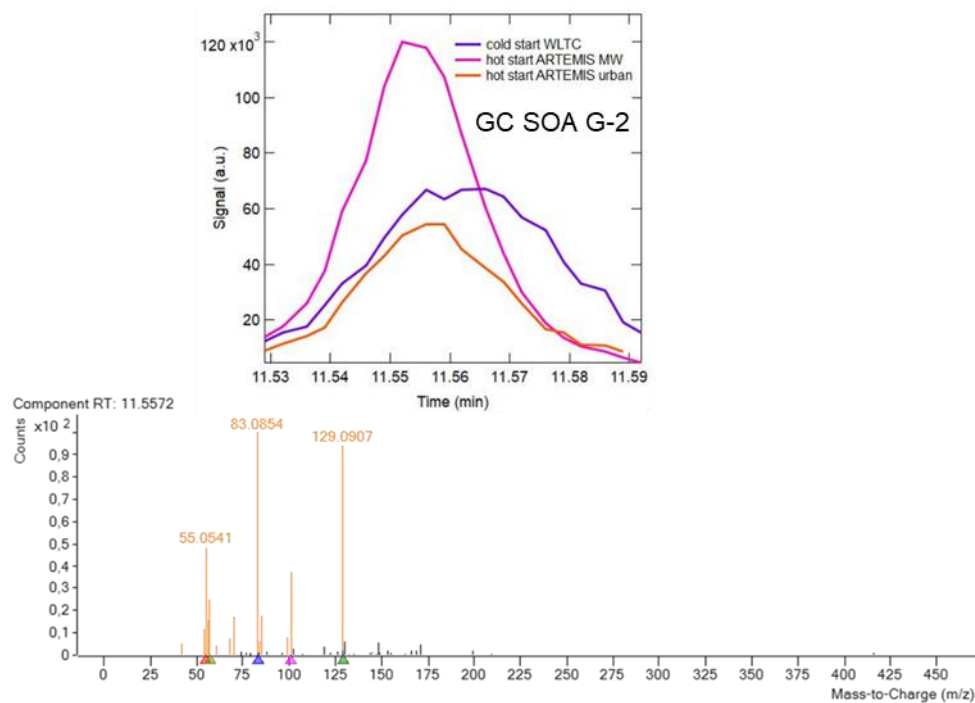
Figure S31. Chromatographic response of the feature base peak (m/z = 129.0909) and the EI mass spectra of one SOA gasoline marker GC SOA G-2 from GC-QToF data (acquisition started at 40 m/z).

45